Tectonophysics, 111 (1985) 173–246
Elsevier Science Publishers B.V., Amsterdam – Printed in The Netherlands

SAUDI ARABIAN SEISMIC-REFRACTION PROFILE: A TRAVELTIME INTERPRETATION OF CRUSTAL AND UPPER MANTLE STRUCTURE

W.D. MOONEY [1], M.E. GETTINGS [2], H.R. BLANK [2] and J.H. HEALY [1]

[1] *U.S. Geological Survey, Menlo Park, CA 94025 (U.S.A.)*

[2] *U.S. Geological Survey, Jiddah (Saudi Arabia)*

(Received September 30, 1983; revised version accepted August 14, 1984)

ABSTRACT

Mooney, W.D., Gettings, M.E., Blank, H.R. and Healy, J.H., 1985. Saudi Arabian seismic-refraction profile: a traveltime interpretation of crustal and upper mantle structure. *Tectonophysics*, 111: 173–246.

The crustal and upper mantle compressional-wave velocity structure across the southwestern Arabian Shield has been investigated by a 1000-km-long seismic refraction profile. The profile begins in Mesozoic cover rocks near Riyadh on the Arabian Platform, trends southwesterly across three major Precambrian tectonic provinces, traverses Cenozoic rocks of the coastal plain near Jizan, and terminates at the outer edge of the Farasan Bank in the southern Red Sea. More than 500 surveyed recording sites were occupied, and six shot points were used, including one in the Red Sea.

Two-dimensional ray-tracing techniques, used to analyze amplitude-normalized record sections indicate that the Arabian Shield is composed, to first order, of two layers, each about 20 km thick, with average velocities of about 6.3 km/s and 7.0 km/s, respectively. West of the Shield–Red Sea margin, the crust thins to a total thickness of less than 20 km, beyond which the Red Sea shelf and coastal plain are interpreted to be underlain by oceanic crust.

A major crustal inhomogeneity at the northeast end of the profile probably represents the suture zone between two crustal blocks of different composition. Elsewhere along the profile, several high-velocity anomalies in the upper crust correlate with mapped gneiss domes, the most prominent of which is the Khamis Mushayt gneiss. Based on their velocities, these domes may constitute areas where lower crustal rocks have been raised some 20 km. Two intracrustal reflectors in the center of the Shield at 13 km depth probably represent the tops of mafic intrusives.

The Mohorovičić discontinuity beneath the Shield varies from a depth of 43 km and mantle velocity of 8.2 km/s in the northeast to a depth of 38 km and mantle velocity of 8.0 km/s depth in the southwest near the Shield–Red Sea transition. Two velocity discontinuities occur in the upper mantle, at 59 and 70 km depth.

The crustal and upper mantle velocity structure of the Arabian Shield is interpreted as revealing a complex crust derived from the suturing of island arcs in the Precambrian. The Shield is currently flanked by the active spreading boundary in the Red Sea.

0040-1951/85/$03.30

INTRODUCTION

A large-scale deep seismic refraction profile across the Arabian Shield and coastal plain of the Kingdom of Saudi Arabia was proposed in 1974 by the geophysics group of the U.S. Geological Survey Saudi Arabian Mission/Directorate General of Mineral Resources (USGS/DGMR). The refraction profile constitutes part of a larger program to delineate the crustal structure and tectonic framework of a 150-km-wide strip transecting the major tectonic, structural, and lithologic provinces of the Arabian Shield. This program, colloquially referred to as the "geophysical strip" (Fig. 1), was an integrated aeromagnetic, gravitational, electrical, electromagnetic, and seismic velocity investigation of the crust along the strip. To better constrain the interpretations, an area was chosen for which there are reasonably complete sets of high-quality geologic maps at 1 : 100,000, 1 : 250,000, and 1 : 500,000 scales.

The refraction profile extends for about 1000 km, approximately down the center of the strip; it is roughly parallel to the southeastern boundary of the Shield and roughly perpendicular to other first-order structural boundaries (Fig. 1). It starts west of Riyadh at the northeastern end, in the rocks of the Mesozoic sedimentary platform and then traverses the Al Amar–Idsas fault zone, the Shammar, Najd, and Hijaz-Asir tectonic provinces (Greenwood et al., 1980), the exposed western margin of the continental plate at the foot of the Asir escarpment, and almost all of the eastern Red Sea shelf, from coastal plain to axial trough in the southern Red Sea.

The profile was designed primarily to obtain information on the thickness, structure, and bulk composition of crustal layers to the depth of the Mohorovičić discontinuity (40 km or more), information which could then be correlated with geologic and other geophysical data. The profile parameters were chosen to yield data that would allow us to examine fundamental questions concerning the late Proterozoic cratonization and tectonic evolution of the Arabian Shield, the origin and significance of tectonic, magmatic, and metallogenic provinces of the Shield, and the nature of a continental-plate margin in an active spreading zone. In addition to its intrinsic importance, a thorough understanding of the tectonic framework of Saudi Arabia is essential to the development of strategies for mineral exploration.

One hundred new portable seismographs were developed by the USGS—Menlo Park for use on the Saudi Arabian seismic deep-refraction profile. Each of the cassette-tape recording units was equipped with an internal crystal clock and a programmable automatic-turnon device, such that they could easily be deployed successively in each of five 200-km recording spreads. A portable computer center, which included a field tape playback, digitizer, and plotting system, was moved along the profile to provide rapid feedback of data quality and content and to allow for preliminary assessment of scientific results as the experiment progressed (Healy et al., 1982).

Five drill-hole shot points were on land, and the sixth was at the southwestern

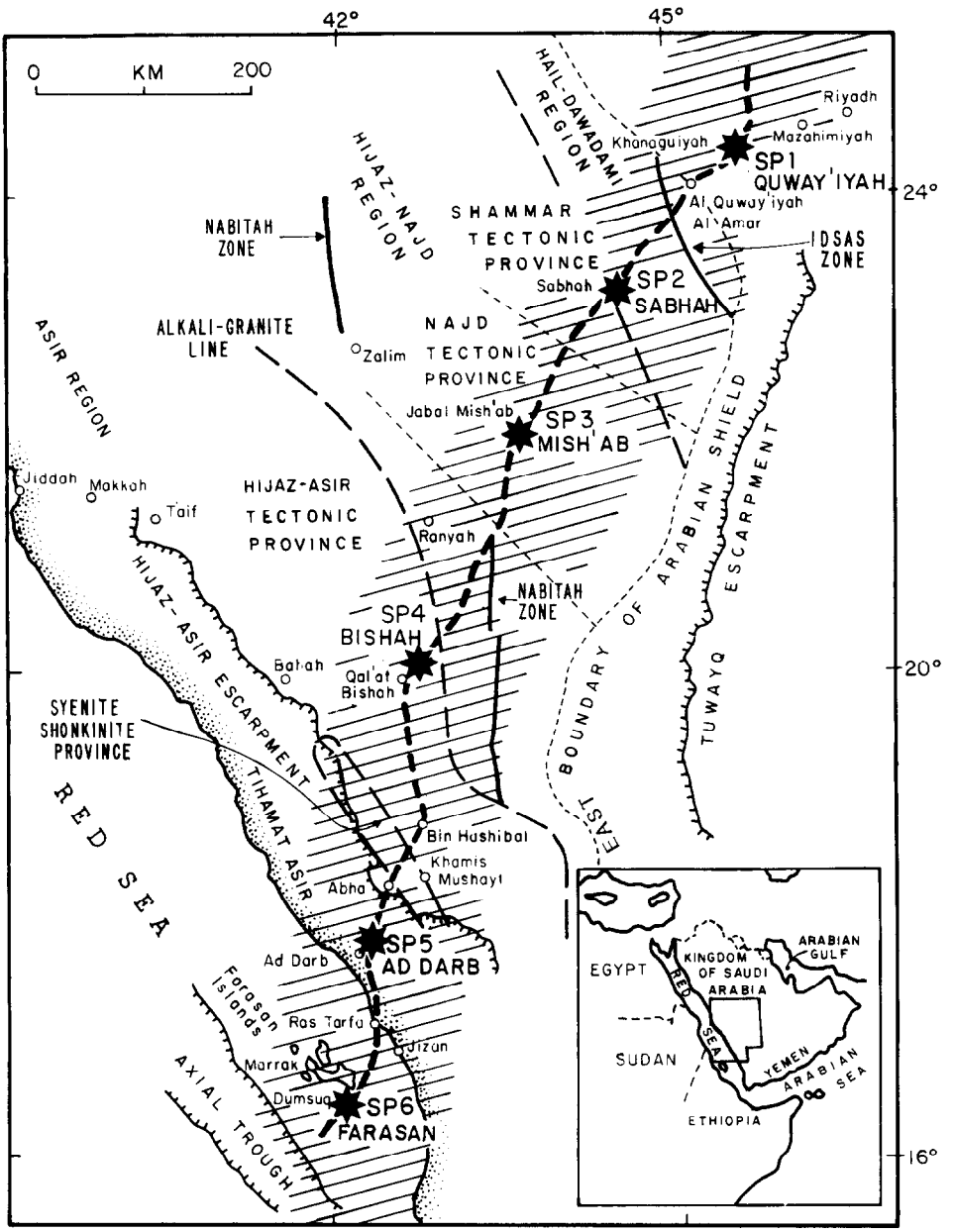

Fig. 1. Map of western Saudi Arabia showing the location of the seismic-refraction profile (shown as dashed line connecting seismic shot points, SP). Hatchured area indicates the area included in the "geophysical strip", as discussed in the text. Tectonic provinces shown are from Greenwood et al. (1980). Petrologic regions and boundaries from Stoeser and Elliott (1980). Nabitah and Idsas zone from Schmidt et al. (1979).

end of the profile in the Red Sea, where explosives on the ocean bottom were detonated from a ship (Fig. 1). Temperature profiles were logged in the drill holes immediately before explosives were loaded. Shot arrivals and seismicity were also recorded at five portable recorder stations on the Red Sea coastal plain (Merghelani and Gallanthine, 1980). The temperature logging and the coastal-plain project were executed by the geophysics group of the DGMR.

Other reports on the seismic refraction profile precede this one. Blank et al. (1979) summarized the experimental procedure and gave a preliminary evaluation of the data. Healy et al. (1982) presented final large-scale copies of the seismic record sections, a complete description of the experiment, and a traveltime interpretation based on preliminary record section plots of the data. In the present report we summarize the main results given by Healy et al. (1982), and utilize their final record sections to develop a somewhat refined traveltime interpretation of the crustal structure. Finally, Gettings et al. (1983, 1985) present an integrated geophysical interpretation of the crustal structure, Prodehl (1985, this volume) presents an interpretation of the entire profile, and Milkereit and Flüh (1985, this volume) interprete the southwestern end of the profile.

GEOLOGIC SETTING AND GEOPHYSICAL DATA

Overview

The seismic deep-refraction profile mostly traverses the Arabian Shield (Fig. 1), which consists predominantly of Precambrian (1.2–0.7 b.y.) metamorphic and plutonic rocks and forms the western one-third of the Arabian Peninsula (Brown, 1972). Greenwood et al. (1980) and Schmidt et al. (1979) divided the Arabian Shield in this area into several tectonic provinces, which include, from northeast to southwest, the Shammar, Najd, and Hijaz-Asir; the latter province is bounded on the southwest by the Hijaz-Asir escarpment. These provinces and the fault zones that bound them are shown in Fig. 1.

The Shield is thought to have evolved from island arcs that formed during a series of subduction episodes and were subsequently juxtaposed by compressional orogenies (Schmidt et al., 1979). To the east, the Shield is bounded by the Mesozoic sedimentary rocks of the Phanerozoic Arabian Platform, which dip gently eastward and overlap the Shield unconformably (Powers et al., 1966). To the west, the Shield abuts the Tertiary rocks at the eastern edge of the Red Sea seafloor spreading system. This tectonic boundary is characterized by complex faulting and Tertiary dike injection and volcanism.

Gettings et al. (1983, 1985) described in detail the geology of the study area and consider existing aeromagnetic (Andreasen et al., 1980) and regional gravity data (Gettings, 1981) for the entire seismic profile. Gettings (1982) and Gettings and Showail (1982) reported on the heat flow measurements made at shot points 1–5.

Previous seismic work

No seismic deep-refraction data have previously been obtained for southwestern Saudi Arabia. Studies of shear waves on the path Addis Ababa-Shiraz, which passes through the Afar depression, show that the average crustal thickness for this region is about 35 km (Niazi, 1968; Knopoff and Fouda, 1975). Shear-wave velocity models from these studies show a pronounced low-velocity zone, the top of which is at a depth of 100–140 km (Knopoff and Fouda, 1975). Although phase velocities of the Arabian Shield are lower than those of the Canadian Shield, they are higher than those of the United States Gulf Coastal Plain (Knopoff and Fouda, 1975).

Girdler (1969) reviewed early seismic work in the Red Sea, which included pioneering surveys made in 1958, using the two ships R.V. "Vema" and R.V. "Atlantis". These surveys included 15 refraction profiles in the northern, central, and southern sectors (Drake and Girdler, 1964). Profiles 170–176 of this set, in the southern sector, show a sedimentary cover, 0.5–4.5 km thick and with a velocity of 3.49–4.48 km/s that consists mostly of the Miocene evaporite-clastic deposits. A profile near the center of the axial trough southwest of the Farasan Islands shows basement velocities of 7.16–7.31 km/s, whereas two profiles on the southern shelves, one west of the axial trough at lat. 16.5°N. and one east of the axial trough at lat. 15°N., show basement velocities of 5.5–5.9 km/s. Elsewhere in the Red Sea the surveys obtained similar results; velocities over the axial trough were mostly in the range 6.8–7.3 km/s, and velocities over the main trough were mostly in the range 5.8–6.1 km/s. However, velocities on the shelves (at lat. 23°–23.5°N.) were as high as 6.97 km/s. Girdler interpreted the high-velocity basement in the axial trough as oceanic crust and the lower velocity basement on the shelves as continental material. In oceanic basins, the arithmetic-mean seismic P-wave velocity of layer two, the upper layer of oceanic crust, is only about 5.1 km/s, with a standard deviation of 0.6 km/s (Hill, 1957; Raitt, 1963; cited in Le Pichon et al., 1973); therefore, if velocities for oceanic crust of Tertiary age are not greatly different from the arithmetic-mean figures, then the lower velocity basement reported by Girdler could be either oceanic or continental.

Other early seismic work in the Red Sea included continuous ("sparker") reflection profiles made by the R.V. "Chain", over the main and axial troughs in 1964 (Knott et al., 1966) and 1966 (Phillips and Ross, 1970) and refraction profiles made using sonobuoys from the R.R.S. "Discovery", on the shelf of the northern sector in 1967 and by the M.V. "Assab", in the central sector in 1967–1968 (Tramontini and Davies, 1969). The M.V. "Assab" survey, which covered a limited area in detail, mainly over the axial trough between lat. 22° and 23°N, shows an average basement velocity of 6.6 km/s and an average basement depth of 4.6 km for that part of the main trough adjacent to the axial trough. The refraction results obtained by the "Discovery" survey are similar to those obtaind by the "Vema"–"Atlantis" survey in 1958.

During the past several years, the Saudi Arabian–Sudanese Joint Commission for Exploitation of Red Sea Mineral Resources has carried out an important series of geophysical investigations in the Red Sea. These investigations include seismic refraction, magnetic, gravimetric, and bathymetric surveys, and the results have apparently not yet been published. Also, cooperative refraction programs, including those of the University of Hamburg with Cairo University and the University of Hamburg with King Abdulaziz University, are being undertaken in the northern Red Sea and adjacent land areas.

In summary, seismic refraction data available from previous surveys on the Red Sea clearly indicate that material having oceanic crustal velocities is present in the axial trough and that the basement of the main trough is composed, at least in part, of oceanic crust. Whether continental crust also underlies the thick sediments on the shelves is controversial. Very little information has been obtained on velocities or crustal thicknesses beneath the landward portion of the shelves, primarily because of the difficulty of navigation in shallow reef zones.

During 1963, the French petroleum company AUXIRAP conducted seismic reflection studies in the seaward portion of the coastal plain in southwest Saudi Arabia (Gillmann, 1968). These studies suggest that the surface of Jurassic and basement rocks dips toward the Red Sea at an average angle of about 10 degrees and that its depth increases from about 2 km some 20 km inland to nearly 5 km in the vicinity of the Mansiyah No. 1 drill hole and Jizan salt dome (the coastline). Unfortunately, the Mansiyah drill hole had to be discontinued just short of where the AUXIRAP studies suggested it would intersect the seismic basement. The profiles did not extend onto the Precambrian Arabian Shield, and the nature of the basement of the Shield remains speculative.

TRAVELTIME INTERPRETATION OF THE REFRACTION PROFILE

Methods

Analysis of the refraction data consisted of the following steps.

(1) Primary and secondary arrivals were determined from the record sections plotted at a reduced velocity of either 6.0 or 8.0 km/s (Healy et al., 1982).

(2) The phases were identified as either refracted or reflected waves based on their amplitudes and traveltime behavior. Once the apparent velocities and time intercepts of the main refractors were identified, the slope-intercept method (Steinhart and Meyer, 1961) was used to obtain a starting model. Iterative one-dimensional ray-tracing was then used to fit refracted and reflected phases.

(3) The one-dimensional models (those in which velocity is a function of depth only) for each shot point were combined to make preliminary two-dimensional models between shot points. A modified version of a two-dimensional ray-tracing program (Červený et al., 1977) was used to compare the theoretical traveltimes for these models with the observations.

(4) On the basis of the apparent amplitude relations of the various phases, qualitative judgments were made concerning the relative sharpness of the seismic discontinuities, and these judgments were used to vary the two-dimensional model. For example, in order to shift critical points, sharp boundaries were converted into transition zones.

True-amplitude record sections (Healy et al., 1982) have not been considered at this stage of the interpretation. The refinement of the derived velocity structure, as determined by the calculation of synthetic seismograms is the subject of continuing analysis.

Flat-layer, unreversed models

Calculating flat-layer (one-dimensional) models is only a first step in modeling seismic refraction data. These models are clearly only approximations because they do not take into account lateral changes in velocity, for example, changes resulting from dips and (or) faults. Therefore, although the general features of the crustal structure presented in this section are reasonably accurate, many details will be added in the succeeding section on two-dimensional modeling.

The nomenclature of the phases identified in the data is as follows. "P_g" refers to a phase refracted through the basement, "P_i" to a phase refracted in the middle crust, "P_iP" to a phase reflected from the middle crustal boundary (if more than one such reflections are identified, they are numbered P_iP_1 and P_iP_2), "P_mP" to a phase reflected from the crust–mantle boundary (variously referred to as the Moho, Mohorovičić discontinuity, or M-discontinuity), and "P_n" refracts through the upper mantle. Upper mantle phases that arrive after P_n are numbered and referred to as "P_1" and "P_2".

Shot point 1

Northeast (1 NE; Figs. 2a and 6). This profile is entirely within the Arabian Platform (Fig. 1). The data, recorded to a distance of only about 85 km, reveal low velocities near the surface and an apparent high gradient in the uppermost basement. The apparent velocity of the first arrivals is about 5.9 km/s up to a distance of 40 km, and then becomes about 6.3 km/s (Fig. 2a). There is considerable scatter in first arrival times between 70 and 85 km. One-dimensional modeling does not adequately represent this profile, which traverses a region in which there are strong lateral changes. See Healy et al. (1982) and Gettings et al. (1983) for a discussion of this short profile.

Southwest (1 SW; Figs. 2b and 6). This profile begins in the Arabian Platform and enters the Shield 43 km southwest of the shot point. Data were recorded to a maximum distance of 655 km, nearly across the entire Shield, with clear arrival times

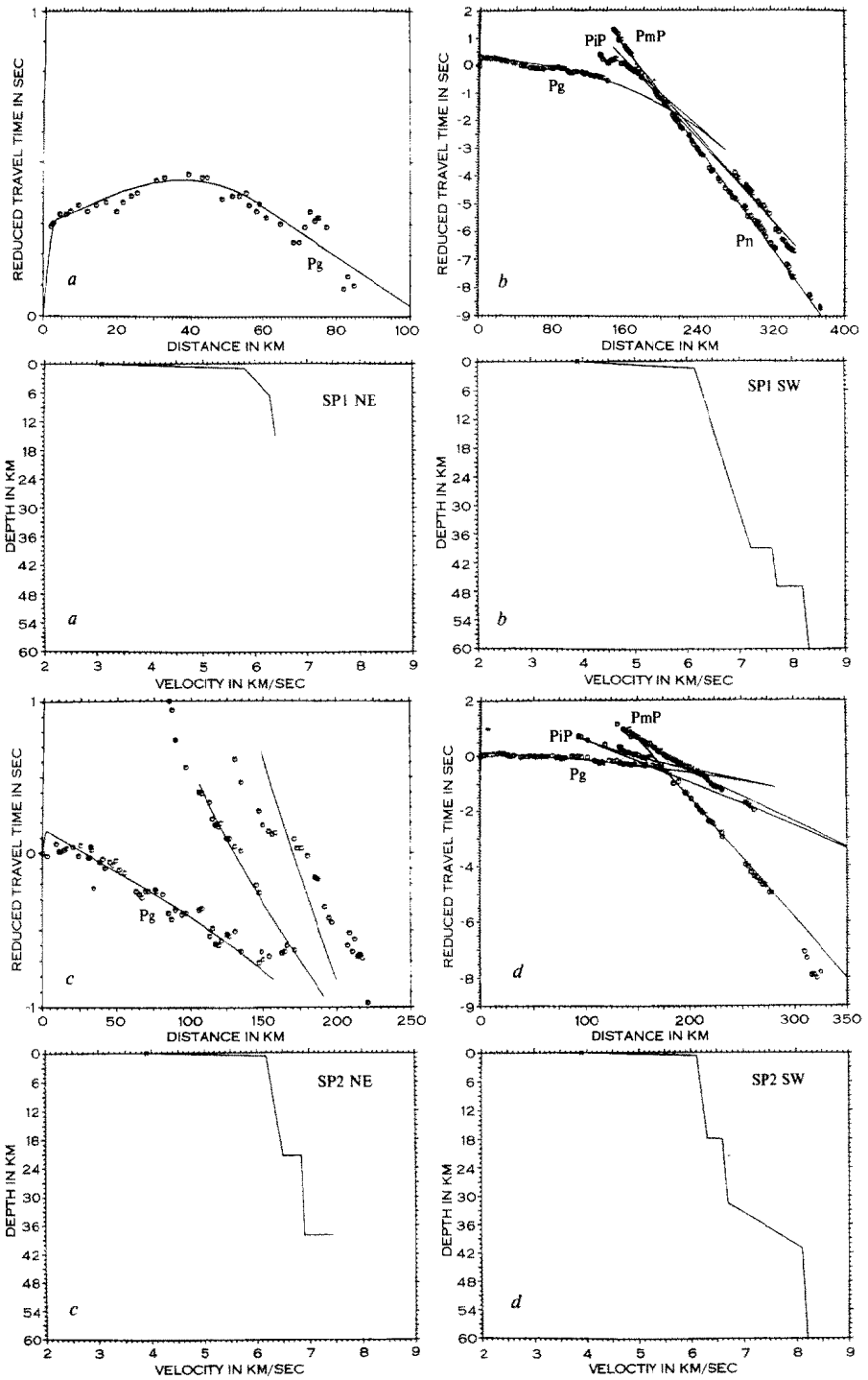

Fig. 2. Flat-layer velocity–depth models for data from shot points: 1 NE (a), 1 SW (b), 2 NE (c), and 2 SW (d). Observed reduced traveltimes are shown as circles in the upper plots with the theoretical reduced traveltimes (solid line) as calculated from the velocity–depth function shown in the lower plot.

to as far away as 550 km. In this discussion we consider only the data to 370 km (Fig. 2b). Low velocities are evident directly beneath the shot point, the basement refractor apparently being at about 1.0 km depth. P_g (basement) arrivals have been fit most accurately between 90 and 150 km. Between 20 and 80 km the arrivals appear to be traveling through a medium that has a higher average velocity than that beyond 90 km. The change to higher velocity occurs near the point at which the profile crosses the Al Amar–Idsas fault (Fig. 1). Between 136 and 180 km clear arrivals are seen as intermediate in time between the P_g and P_mP/P_n phases. We refer to these phases as P_iP if we believe them to be reflections from an intermediate crustal boundary and as P_i if we believe them to be refractions from that boundary. In order to fit the high apparent velocity of these P_iP arrivals, we used a continuous velocity gradient increasing from 6.15 km/s at 1.5 km depth to 7.2 km/s at 39 km depth. A discontinuity occurs at 39 km depth where the velocity increases to 7.6 km/s. Below 39 km, the velocity increases slowly until it reaches 7.7 km/s at 47 km depth, the crust–mantle boundary. The best fitting P_n velocity is 8.15 km/s at 47 km depth. The velocity model is unique among the Shield profiles in that it lacks a velocity discontinuity at about 20 km depth; this may be in part result from a lateral change in crustal composition 120 km southwest of shot point 1. This change is discussed more thoroughly in later sections.

Shot point 2

Northeast (2 NE; Figs. 2c and 7). This profile begins in the Shammar tectonic province of the Shield (Greenwood et al., 1980) and enters the platform about 100 km from the shot point. Between the shot point and 150 km the first arrivals (P_g) are fit by use of a velocity gradient in the upper crust ranging from 6.2 km/s at 1 km depth to 6.5 km/s at 21 km depth (Fig. 2c). Between 85 and 150 km clear intermediate arrivals (P_iP) are modeled as reflections from a discontinuity at 21 km depth, at which the velocity increases from 6.5 to 6.85 km/s. A mantle depth of 38 km matches the average arrival time of presumed mantle (P_mP) arrivals but fails to match the low apparent velocity of this phase. Both the velocity model for this profile and that of shot point 1 SW (Fig. 2b) indicate a velocity discontinuity at about 38 km depth, but neither clearly indicates that it is the M-discontinuity. The discontinuity suggests either a dip in the Moho or that a high-velocity lower crustal layer is present between shot points 1 and 2.

Southwest (2 SW; Figs. 2d and 8). This profile, as well as the next four discussed, was recorded entirely within the Arabian Shield; it crosses three tectonic provinces and the faults that separate them. The data on this profile have some of the highest signal-to-noise ratios of all data recorded during the project (Fig. 8). The flat-layer model was very successful in modeling the arrival times of both primary and secondary phases. P_g is modeled with a velocity gradient from 6.1 km/s at 1 km

depth to 6.3 km/s at 18 km depth (Fig. 2d). This upper crustal velocity structure is remarkably different from those of the previous three profiles discussed, all of which indicate significantly higher velocities. The data from shot point 1 SW, for example, have a traveltime that is 0.25 s faster at a distance of 140 km than the data from shot point 2 SW. Intermediate crustal arrivals are modeled as reflections (P_iP) from a discontinuity at 18 km depth.

The profile provides crucial evidence that the M-discontinuity in this region is not a first-order discontinuity but rather is transitional. The evidence includes the approximate 150-km critical distance for the P_mP arrivals, the high amplitudes of the postcritical P_mP arrivals, and the low amplitudes of the precritical P_mP arrivals. In this one-dimensional calculation the transition from the crust to the mantle is modeled as occurring between 31.5 and 41 km depth, with the velocity increasing from 6.7 to 8.1 km/s. Clearly, comparison of synthetic seismograms with the true-amplitude record sections presented in Healy et al. (1982) is needed to examine the validity of this structure. In part because of the data on this profile, a crust–mantle transition zone (specifically, a velocity gradient followed by a small velocity discontinuity to the mantle) has been incorporated into the two-dimensional raytrace models discussed below. P_n arrivals on this profile have been fit with a mantle velocity that increases from 8.1 km/s at 41 km depth to 8.2 km/s at 60 km depth.

Shot point 3

Northeast (3 NE; Figs. 3a and 9). This short profile was recorded entirely in the Najd tectonic province and crossed no major mapped faults (Fig. 1). Data were recorded to a distance of 56 km and indicate a refraction velocity of 6.0–6.1 km/s with only about 100 m of lower velocity near-surface materials (Fig. 3a). Because the short length of this profile leaves profile 2 SW essentially unreversed, the subsurface structure northwest of shot point 3 is indicated by dashed lines on Fig. 17.

Southwest (3 SW; Figs. 3b, 3c and 9). This profile extends across several important features of the Shield (Fig. 1). It begins in the Najd tectonic province, crosses the southwest Najd fault zone, and enters the Hijaz-Asir tectonic province. Within the latter province, it crosses the Nabitah zone (a region of ultramafic rocks), the Al Qarah gneiss dome, and the Al Junaynah fault zone.

Close to the shot point P_g has an apparent velocity of 6.0 km/s. This apparent velocity is followed at 30 km by an apparent velocity of 6.3 km/s, which continues to 175 km. Intermediate arrivals (P_iP) are clearly observed and are modeled by a discontinuity at 22.5 km depth where the velocity increases from 6.45 to 6.7 km/s (Fig. 3b). The P_mP arrivals are modeled with a sharp M-discontinuity at 35 km depth, where the velocity increases from 6.7 to 8.0 km/s. In light of the low amplitudes of the P_mP reflections, however, it is unlikely that the sharp M-discon-

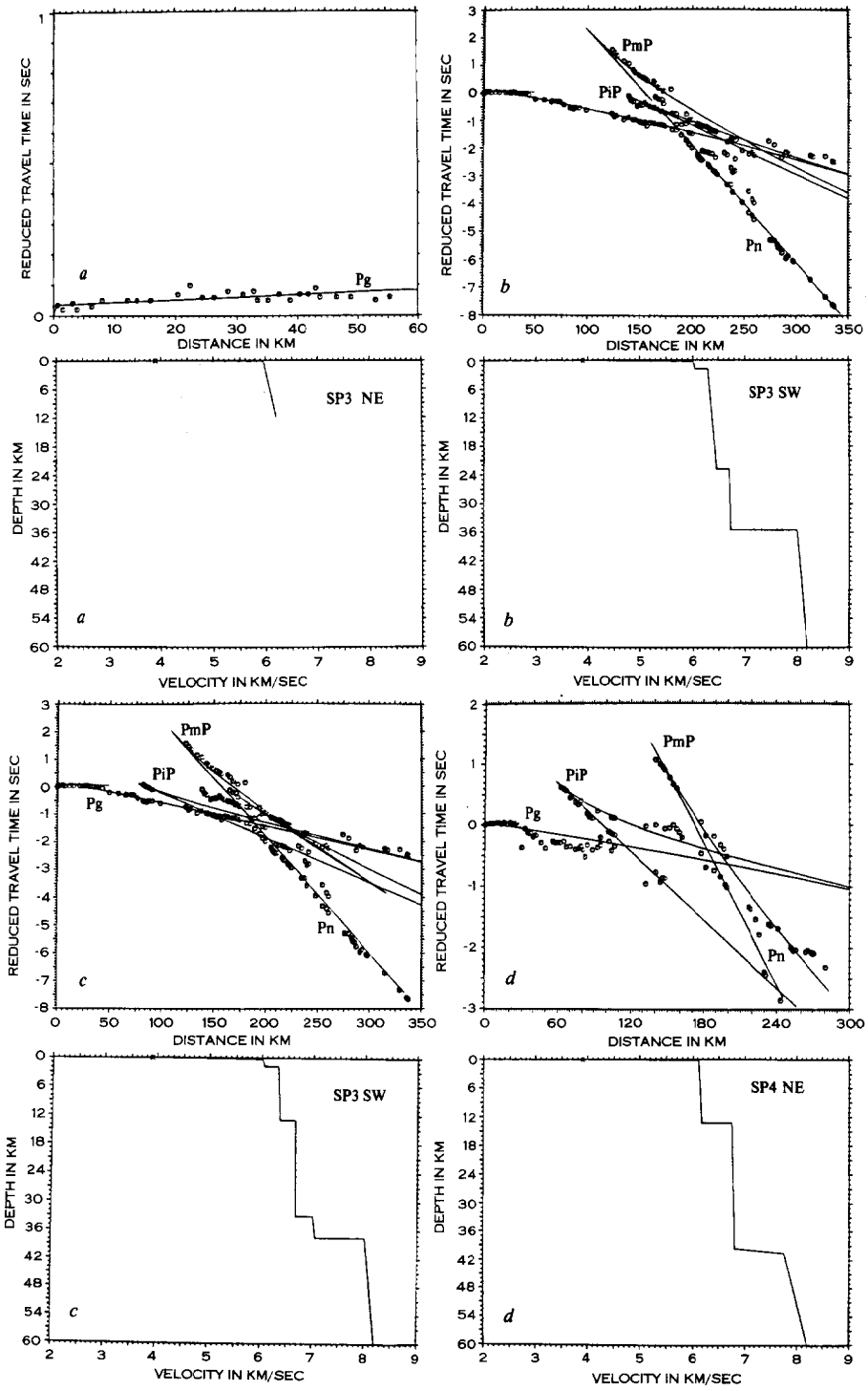

Fig. 3. Flat-layer velocity–depth models for data from shot points: 3 NE (a), 3 SW (b), 3 SW (alternative) (c), and 4 NE (d). Presentation as in Fig. 2.

tinuity is real, and a transition zone has been used in the two-dimensional ray-tracing model (next section). P_n arrivals have been fit by using a positive velocity gradient in the upper mantle of 0.008 km/s/km.

An alternative model for profile 3 SW was made in an attempt to explain some clear secondary arrivals that were observed at a distance of about 85 km at a reduced traveltime of 0.0 s. These are modeled (Fig. 3c) with a discontinuity at 13 km depth, where the velocity increases from 6.35 to 6.65 km/s. Bringing this high velocity to shallow depth makes it difficult to fit other secondary arrivals that are observed between 140 and 175 km at a reduced traveltime of −0.5 s. These secondary P_iP arrivals are important because they appear to be from the boundary between the upper and lower crust. A possible model, as yet untested, is one with a low-velocity zone (LVZ) at 16–21 km depth. A strong reflection that could fit the P_iP arrivals would then occur off the bottom of this zone. The possibility of low-velocity zones is examined further in the "Discussion" section. Both P_mP and P_n arrivals are adequately fit by the mantle depth (37.5 km) and velocity (8.0 km/s) used in this alternative model.

Shot point 4

Northeast (4 NE; Figs. 3d, 4a and 11). This profile starts in the Hijaz-Asir tectonic province and crosses into the Najd province; en route it crosses the Al Junaynah fault zone, the Al Qarah gneiss dome, and the Nabitah zone (Figs. 1, 17). A simple 6.2-km/s refractor fits the data to a distance of 40 km, but beyond this point a traveltime advance of some 0.2–0.3 s is apparent. A laterally varying model is required to fit these traveltimes, which are advanced because of the high-velocity Al Qarah gneiss dome. We propose two models to fit the intermediate arrivals. In the first (Fig. 3d), we assume that two distinct phases are present (P_iP_1 and P_iP_2) and use two intracrustal discontinuities (at 13 and 34 km depth) to fit the arrivals. The Moho is modeled by a discontinuity at 42 km, where the velocity increases from 7.2 to 7.8 km/s. Although this model fits most of the data adequately, the high velocity of the lowermost crust required to fit the P_iP_2 arrivals then causes the theoretical wide-angle P_mP reflection to arrive early. A low-velocity zone beneath the lower crustal discontinuity could explain this. Alternatively, a simpler model (Fig. 4a) associates the P_iP_2 arrivals with wide-angle reflections from a single discontinuity at 13 km depth. In this case, the lower crust has a velocity of about 6.8 km/s, and the wide-angle P_mP phase fits the observations at a distance of 240–280 km. Amplitude modeling would be effective in better resolving these uncertainties in structure.

Southwest (4 SW; Figs. 4b and 12). This profile crosses from the Hijaz-Asir tectonic province to the Red Sea. It reaches the Khamis Mushayt gneiss (about 35 km wide) at a distance of 130 km and the Hijaz-Asir escarpment at about 225 km. The P_g velocity is 6.1 km/s, and arrivals from a mid-crustal reflection (P_iP) are evident at

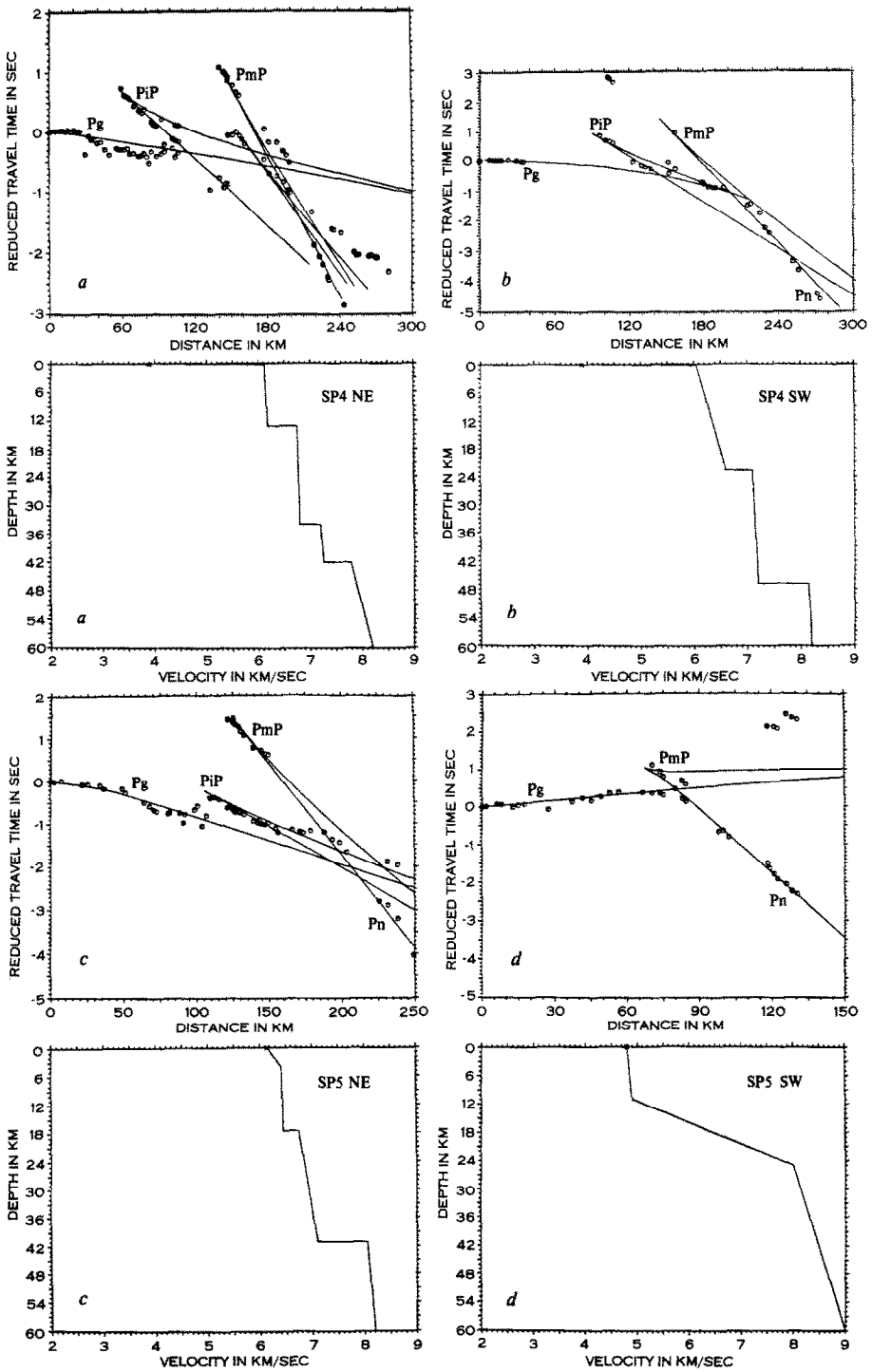

Fig. 4. Flat-layer velocity–depth models for data from shot points: 4 NE (alternative) (a), 4 SW (b), 5 NE (c), and 5 SW (d). Presentation as in Fig. 2.

100 km and beyond (Fig. 4b). These are modeled with a velocity discontinuity at a depth of 23 km, where the velocity increases from 6.6 to 7.1 km/s. It was very difficult to pick additional secondary arrivals with certainty on this profile because of the high dominant frequency throughout the seismograms (Fig. 12). This high frequency may result in part from the low seismic attenuation and high amount of scattering that occurs as the profile crosses the Khamis Mushayt gneiss, which occurs at just the distance where secondary arrivals should be the strongest. The P_n arrivals were fitted with a mantle velocity of 8.15 km/s. All other phases were discontinuous and uncertain.

Shot point 5

Northeast (5 NE; Figs. 4c and 13). This profile begins just northeast of the Tihamat Asir (coastal plain), extends across the Hijaz-Asir escarpment and Khamis Mushayt gneiss, and ends within 9 km of shot point 4 (Figs. 1, 17). The P_g traveltime curve gives unmistakable evidence for high upper crustal velocities (about 6.45 km/s) beginning about 50 km northeast of the shot point (Fig. 4c). This higher velocity persists as the profile passes through the Khamis Mushayt gneiss. Secondary arrivals (P_iP) are evident at a distance of 110–175 km and have been modeled by a discontinuity at 17 km depth, where the velocity increases from 6.45 to 6.75 km/s. P_mP (mantle reflection) arrivals are clear between 120 and 150 km but are very difficult to correlate at greater distances, possibly because the seismic energy passes through a disrupted lower crust beneath the Khamis Mushayt gneiss. The velocity in the lower crust increases from 6.75 to 7.1 km/s between 17 and 41 km depth. The available mantle arrivals (P_mP and P_n) are fit reasonably well with the M-discontinuity at 41 km depth and having a velocity of 8.1 km/s.

Southwest (5 SW; Figs. 4d and 13). This profile crosses the Tihamat Asir and continues onto the Red Sea shelf, where several islands were used as recording sites. At the eastern edge of the Tihamat Asir, the profile crosses a dike complex intruded by gabbros and related rocks; this region may be considered the Red Sea–Shield boundary (Fig. 17). The clearest evidence that these data were recorded in a region of strong lateral variation is given by the P_n apparent velocity of about 9.0 km/s (Fig. 4d). Because this is an unreasonably high velocity for the uppermost mantle, it is obvious that either the crust thins toward the Red Sea, such that the profile shoots up dip, or the average crustal velocity increases rapidly seaward. Despite the evidence that this region has strong lateral velocity variations, the profile was modeled with a flat-layer solution. The basement velocity (P_g) of 5.85 km/s is the lowest observed on any profile in this data set. Because, in view of the local geology, the basement rocks should have a velocity greater than 5.85 km/s, we assume that the P_g apparent velocity is a down-dip measurement, that is, a thickening surficial sedimentary layer. Both the mantle refraction (P_n) and reflection (P_mP) traveltimes

indicate a much thinner crust (about 17.5 km) beneath the coastal plain than that observed on the Shield. The flat-layer velocity model must include a broad transition zone from 5.9 to 8.0 km/s between 11 and 24 km depth (mid-depth 17.5 km) in order to fit the critical reflection point.

Shot point 6

Northwest (Figs. 15 and 16). This profile was not modeled with a flat-layer solution.

Two-dimensional models

Using the results of the flat-layer modeling presented in the previous section, two-dimensional velocity models were constructed for profile sets 3–2–1, 5–4–3, and 6–5. Combining the flat-layer velocity models required subjective decisions about how to make compatible the velocity–depth functions for neighboring shot points. In order to obtain the simplest model consistent with the data, we decided to use as few layers as possible. Specifically, this meant that strictly local features were not included in the two-dimensional ray-trace model, although some such features have been included in the interpretive crustal section (Fig. 17). We expect that this simple model can be elaborated on by the interpretation of the true-amplitude record sections (Healy et al., 1982).

The basic model chosen consists of an upper and lower crust, each having two layers, and a two-layer mantle. In the upper crust, two layers are needed to model both the near-surface rocks, which often have velocities less than 6.0 km/s, and the basement rocks, which have velocities greater than 6.0 km/s. In the lower crust, two layers are needed to model both the region just below the mid-crustal discontinuity (about 20 km deep) and the crust–mantle transition zone. Two mantle layers are used for most of the ray-trace calculations; the first is directly beneath the crust (where the P_n phase propagates), and the second is in the uppermost mantle at about 60 km depth. An additional mantle discontinuity layer at 70 km depth was used to model the data from shot point 6 NE.

Shot points 3–2–1

The profiles from shot points 1, 2, and 3 (Figs. 5–9) cover the transition from the Arabian Platform to the Shield and encompass the Shammar and Najd tectonic zones (Figs. 1, 17). (The model used for the basement along the profile from shot point 1 northeast is as presented in Healy et al. (1982) and Gettings et al. (1983).)

The P_g arrivals from shot point 1 SW match the calculated traveltimes quite closely (Figs. 5a and 6), but the velocity discontinuity at 21 km depth predicts P_iP arrivals about 0.3 s ahead of the observed high-amplitude arrivals. However, the depth to this boundary was not increased because its position provided an excellent fit to the P_iP arrivals recorded on profile 2 NE (Figs. 5b and 7). Therefore, there are

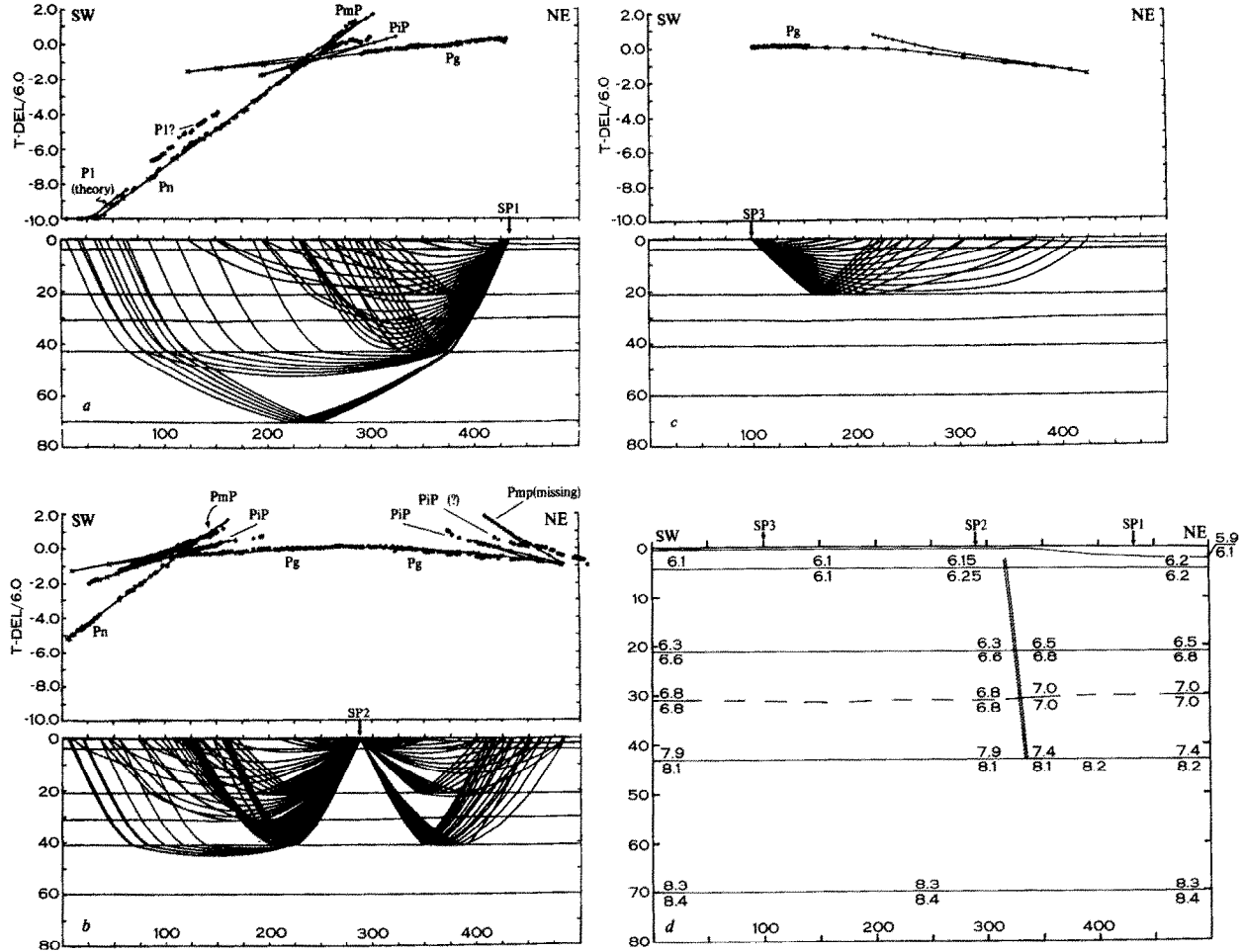

Fig. 5. Two-dimensional ray-trace models for the data from shot point 1 SW (a), 2 NE and 2 SW (b) and 3 NE (c). In the upper portion of each panel the observed reduced traveltimes are shown as solid circles and the calculated reduced traveltimes, obtained by tracing rays through the velocity model (d), are shown as a solid line.

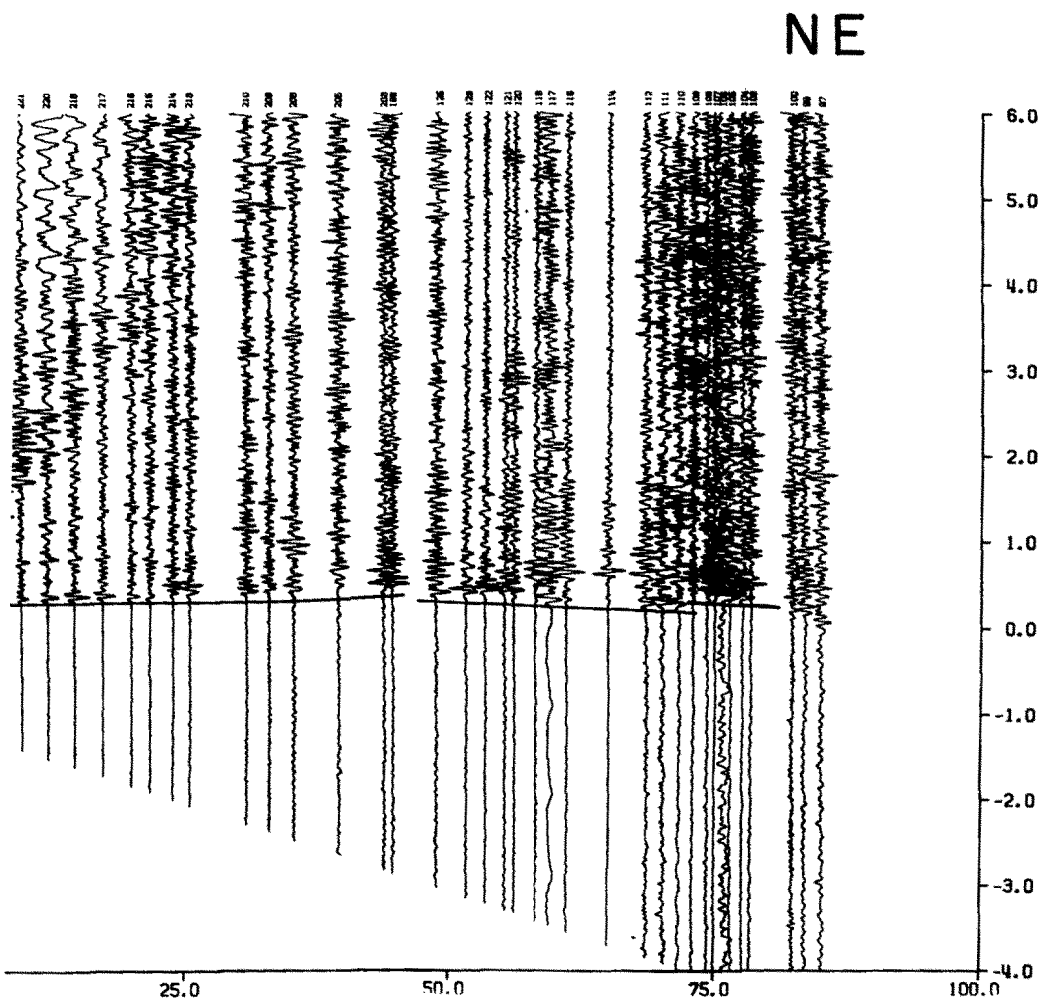
NE
6.0
5.0
4.0
3.0
2.0
1.0
0.0
-1.0
-2.0
-3.0
-4.0
25.0
50.0
75.0
100.0

E (Normalized)

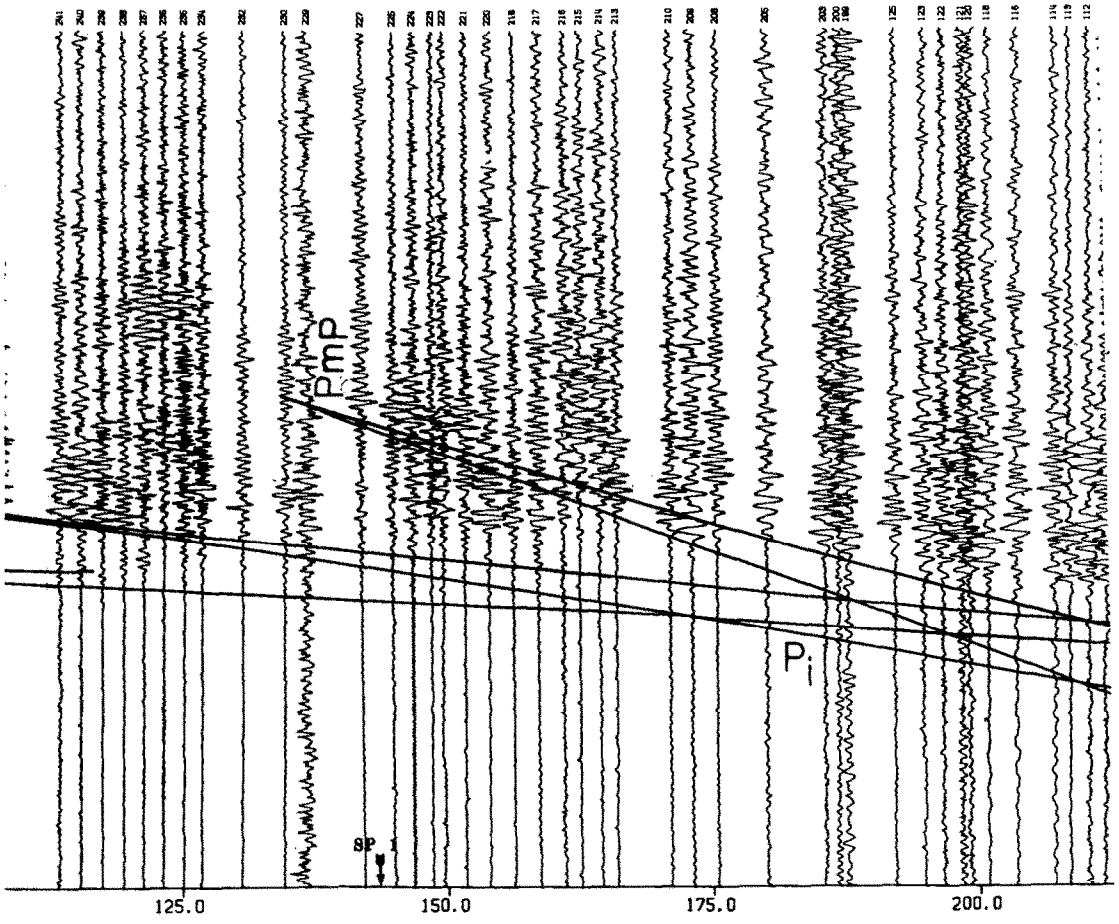

C E (K M)

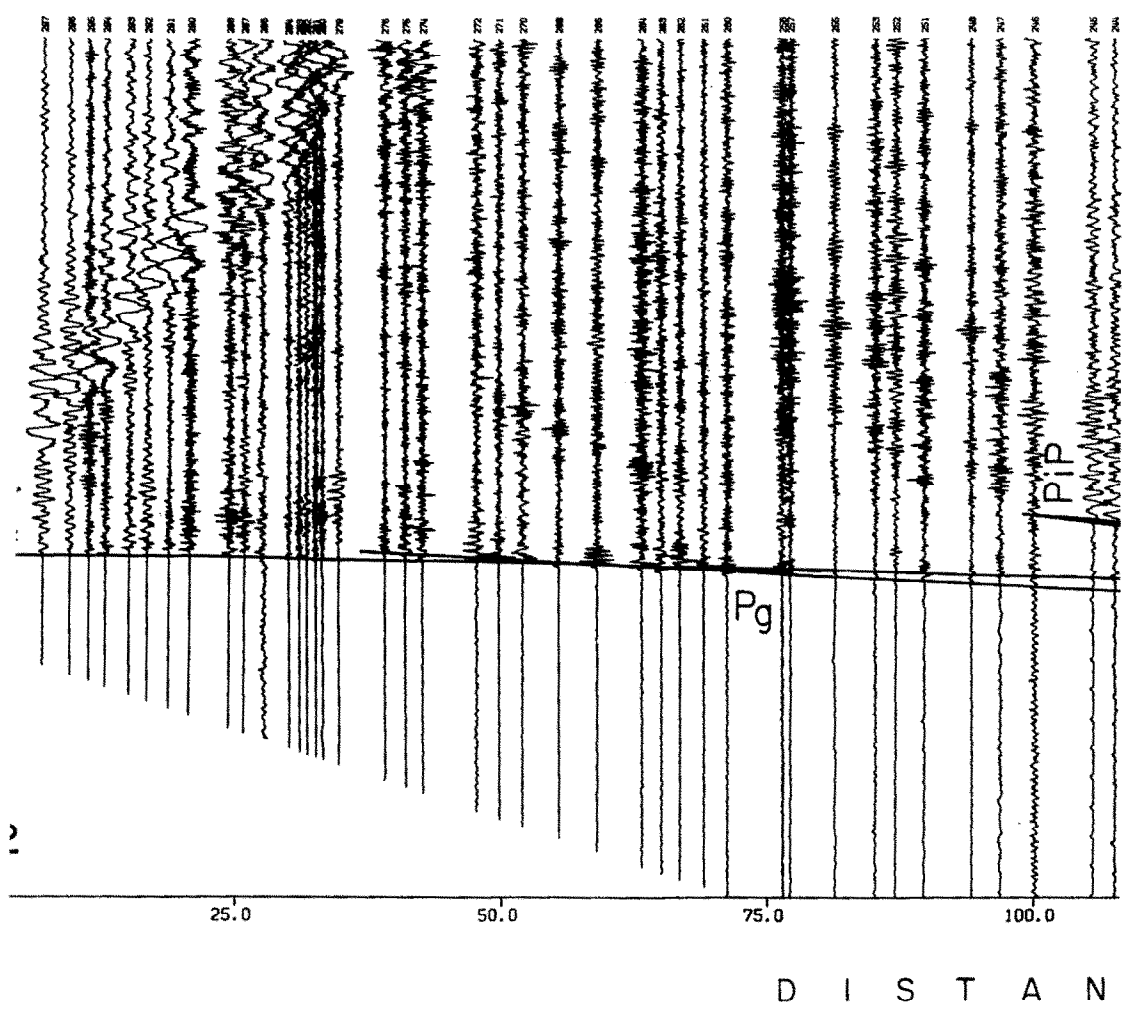

mic record section for the data from shot point 2 NE. Presentation as in Fig. 6.

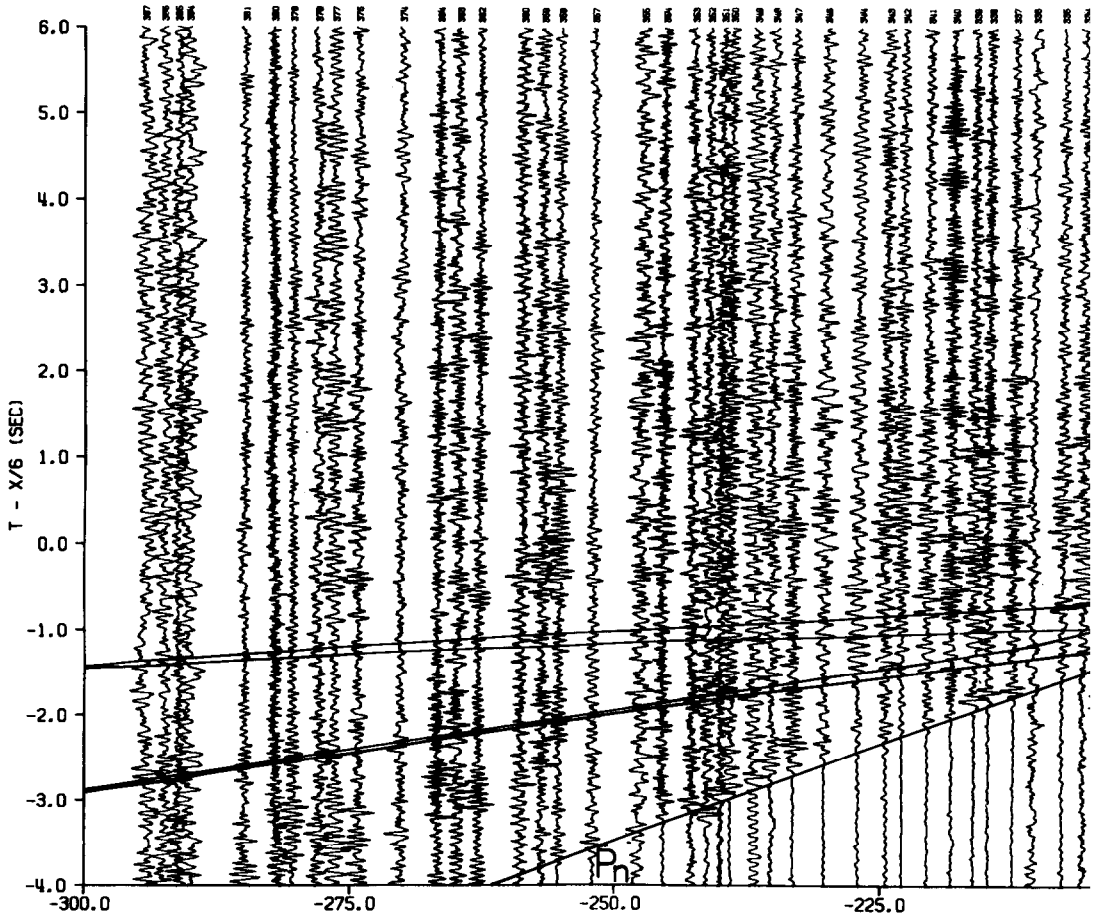

Fig. 6. Seismic record section for the data from shot points 1 NE and 1 SW. A reduction velocity of 6.0 km/s has been applied, and each seismogram has been normalized to the maximum amplitude in the seismogram before plotting. The traveltime curves calculated for shot point 1 in the velocity model of Fig. 5d have been superimposed on the record section.

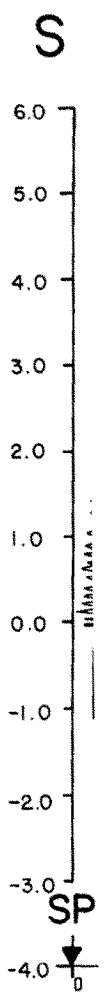

Fig ---

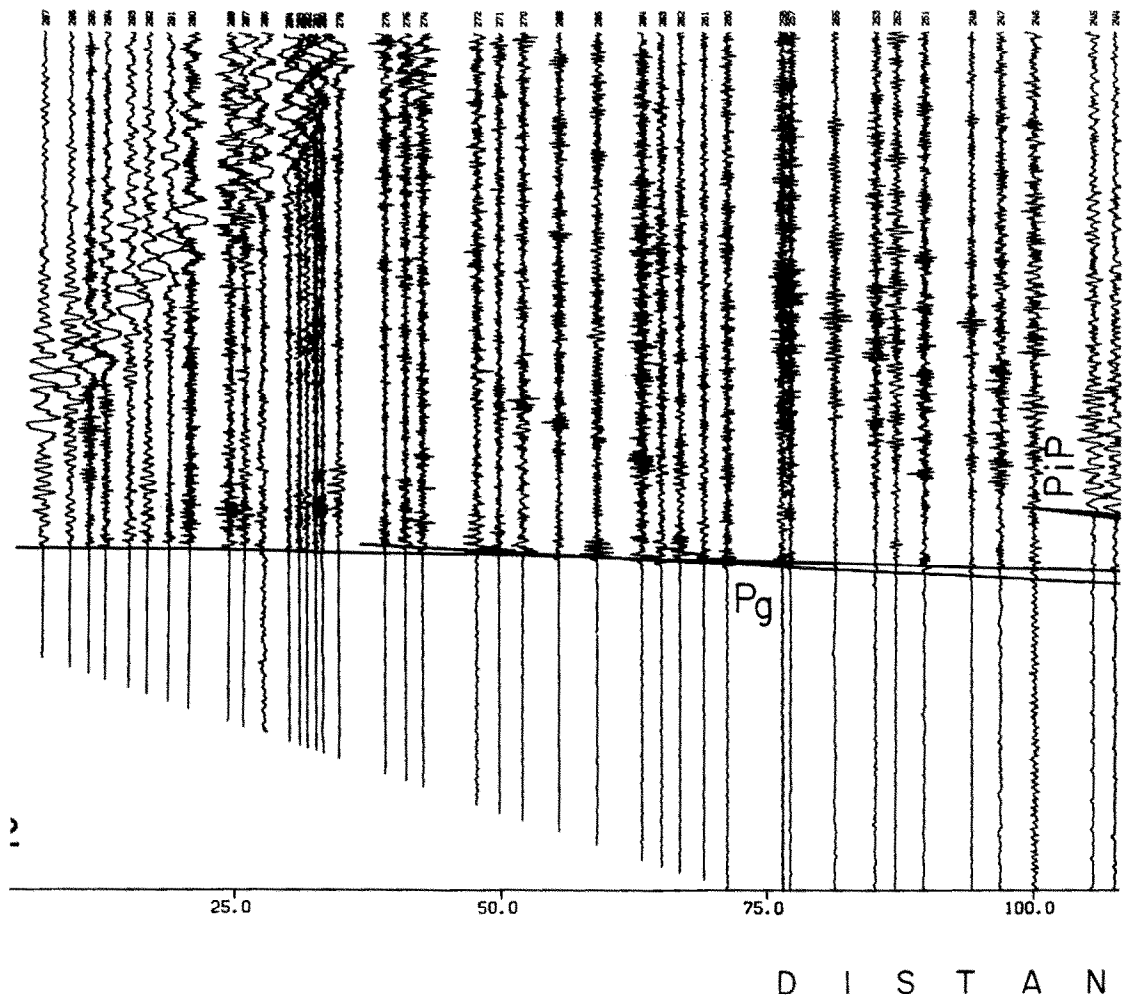

mic record section for the data from shot point 2 NE. Presentation as in Fig. 6.

E (Normalized)

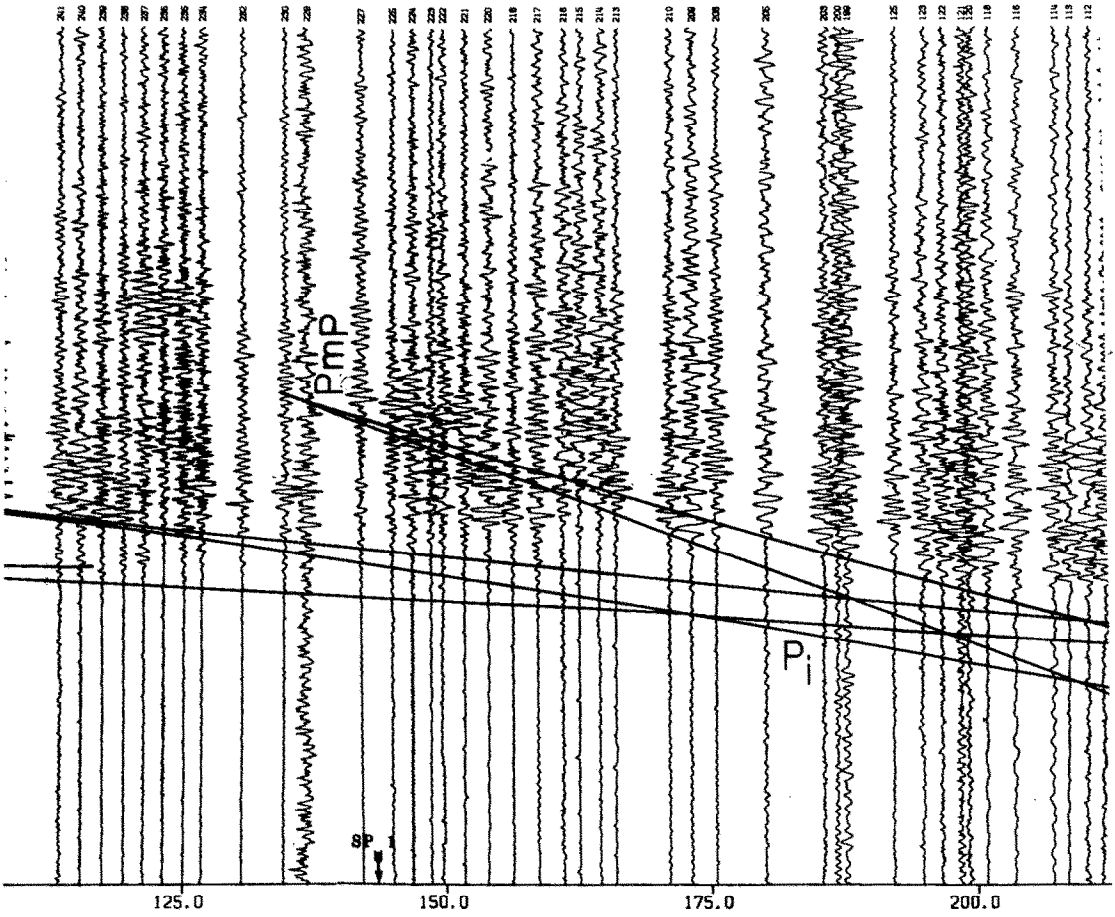

C E (K M)

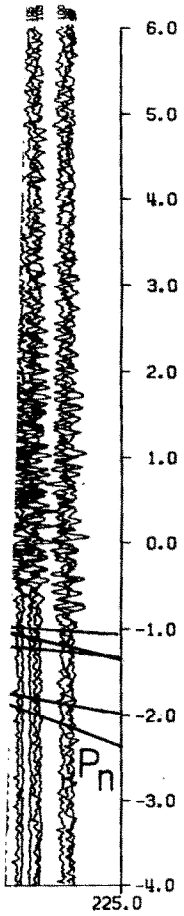
6.0
5.0
4.0
3.0
2.0
1.0
0.0
-1.0
-2.0
Pn
-3.0
-4.0
225.0

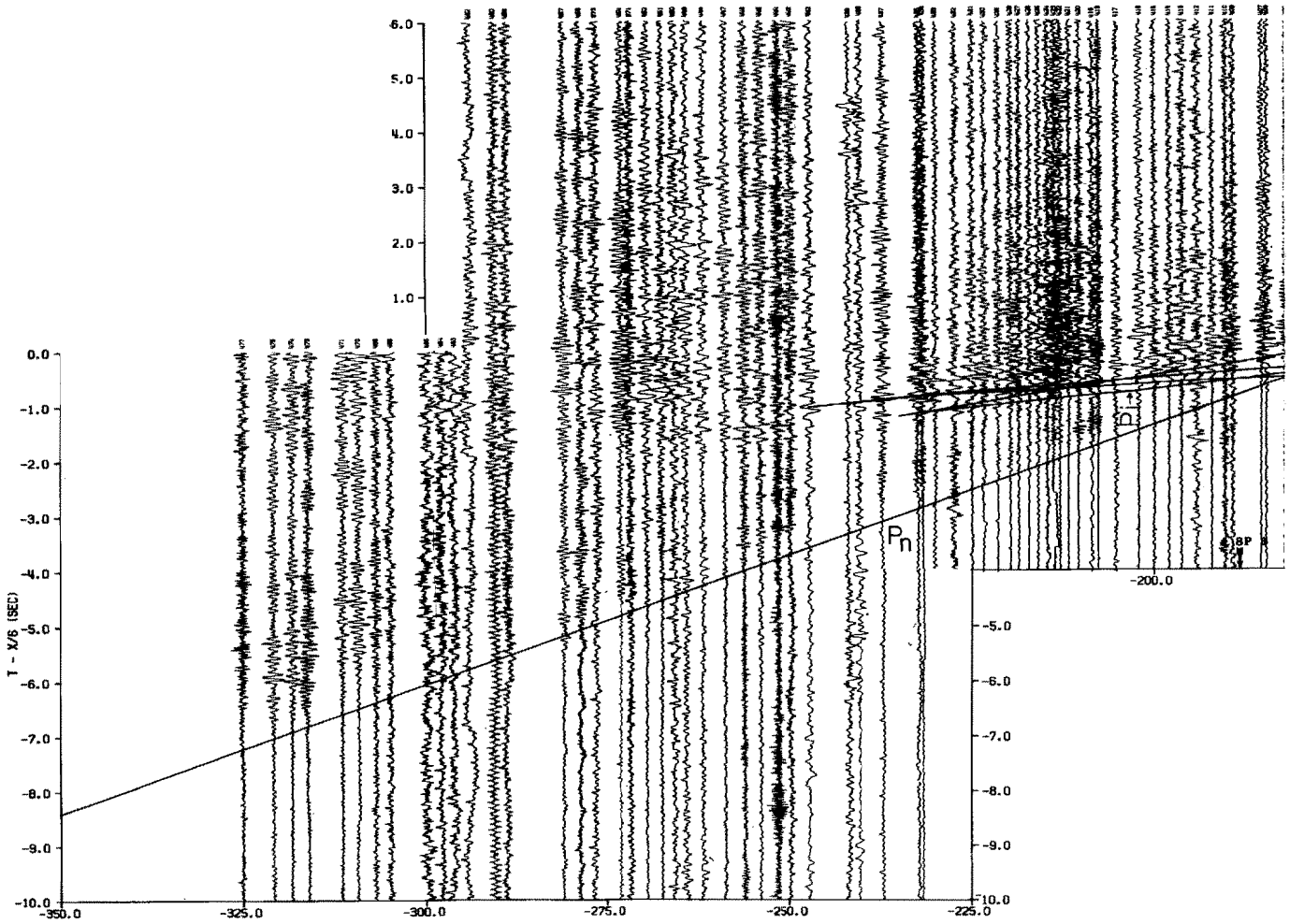

Fig. 8. Seismic record section for the data from shot point 2 SW. Presentation as in Fig. 6.

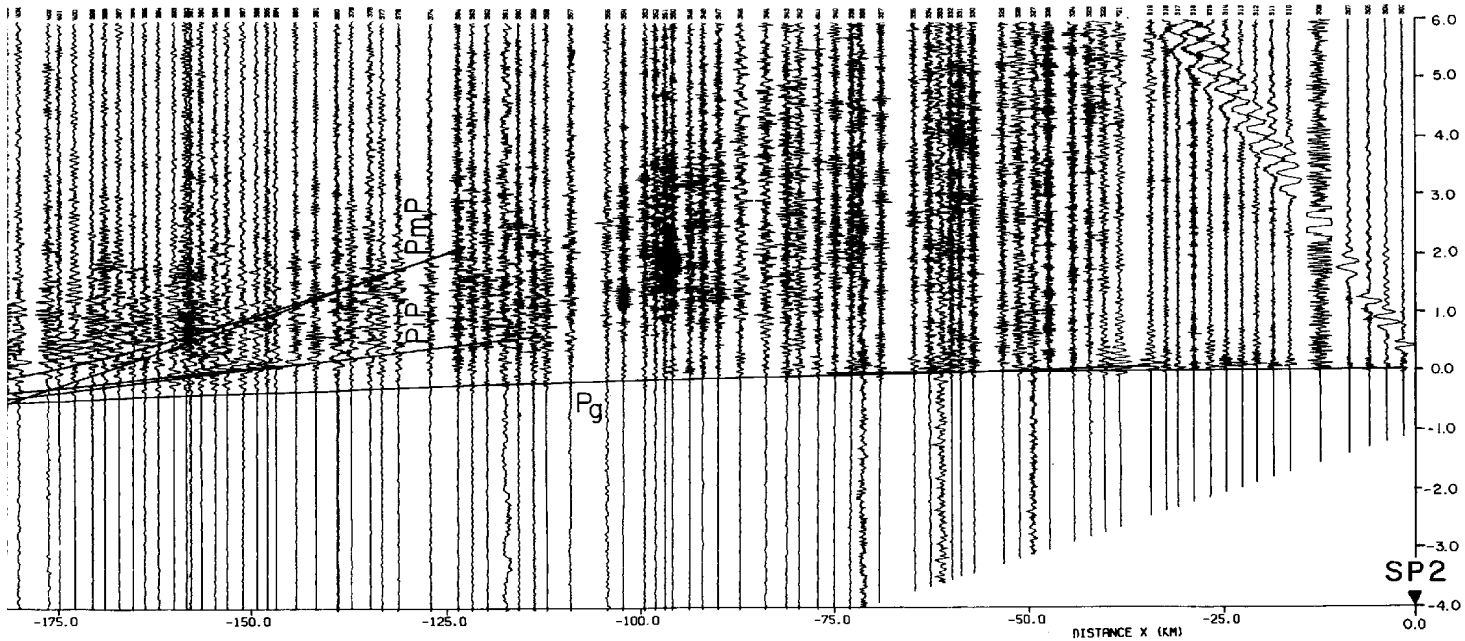
N (Normalized)
PmP
PmP
Pg
SP2
-175.0
-150.0
-125.0
-100.0
-75.0
-50.0
-25.0
0.0
DISTANCE X (KM)
6.0
5.0
4.0
3.0
2.0
1.0
0.0
-1.0
-2.0
-3.0
-4.0
DISTANCE (KM)

pp. 201–204

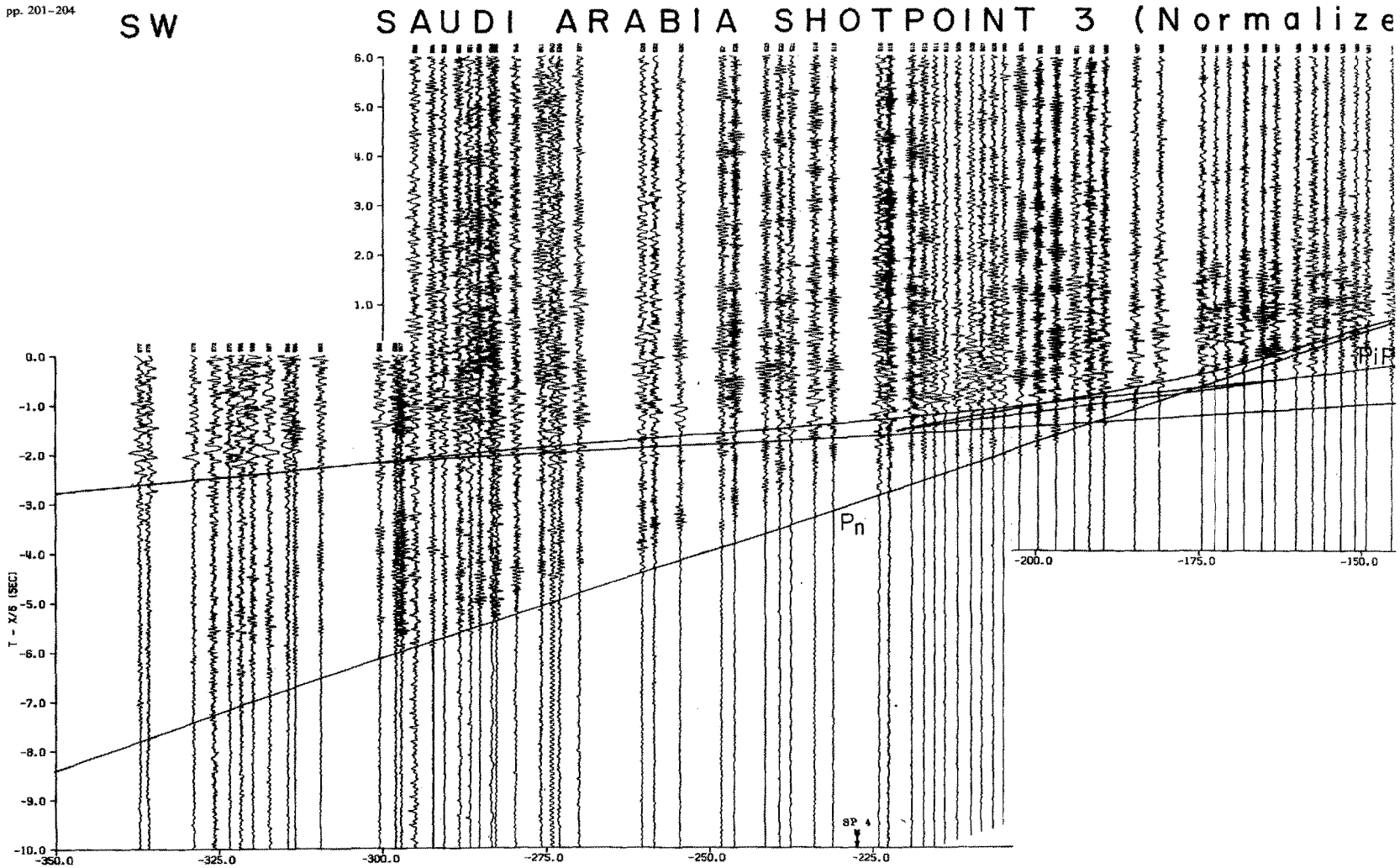

Fig. 9. Seismic record section for the data from shot points 3 NE and 3 SW. Presentation as in Fig. 6.

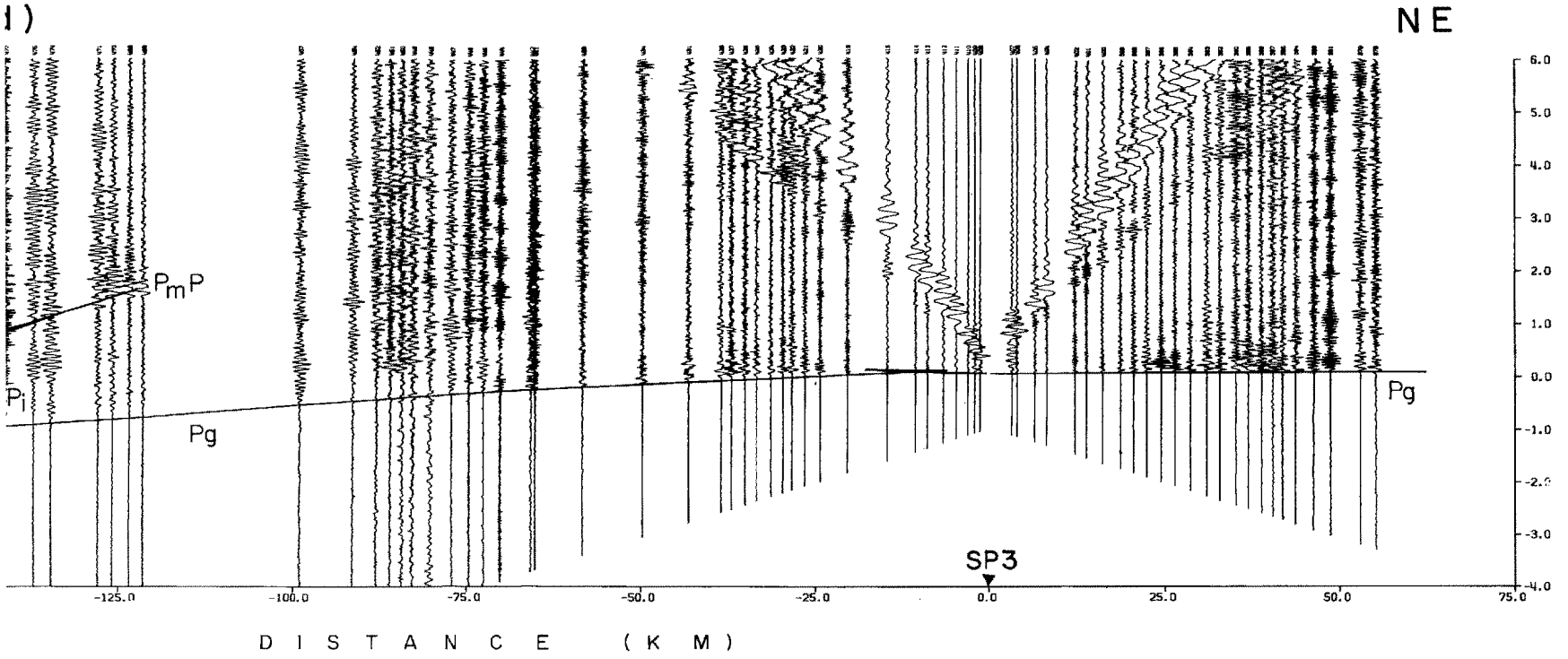
1)
NE
PmP
Pi
Pg
Pg
SP3
-125.0
-100.0
-75.0
-50.0
-25.0
0.0
25.0
50.0
75.0
6.0
5.0
4.0
3.0
2.0
1.0
0.0
-1.0
-3.0
-4.0
DISTANCE (KM)

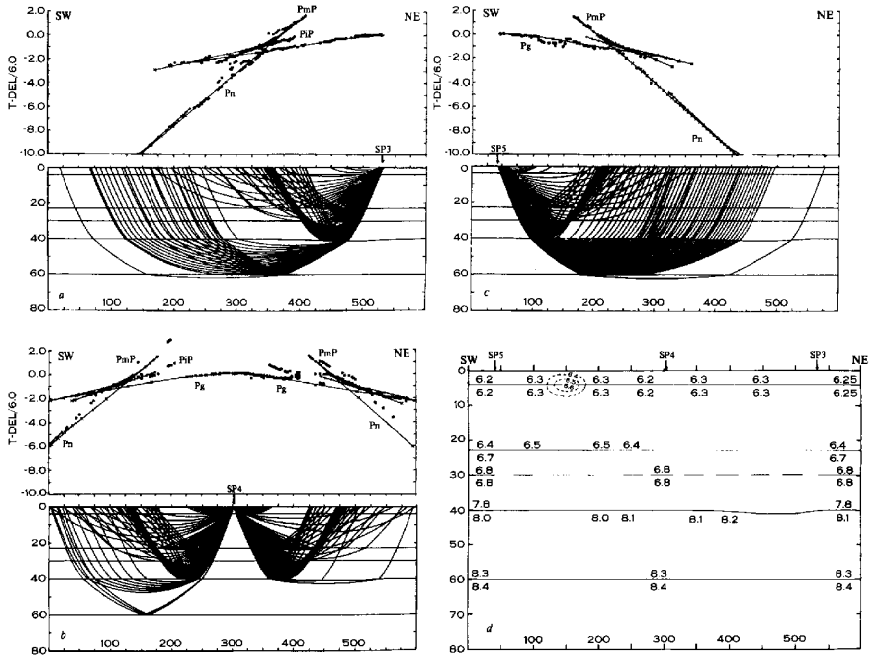

Fig. 10. Two-dimensional ray-trace models for the data from shot points 3 SW (a), 4 NE and 4 SW (b), and 5 NW. Presentation as in Fig. 5. The velocity model is shown in panel (d).

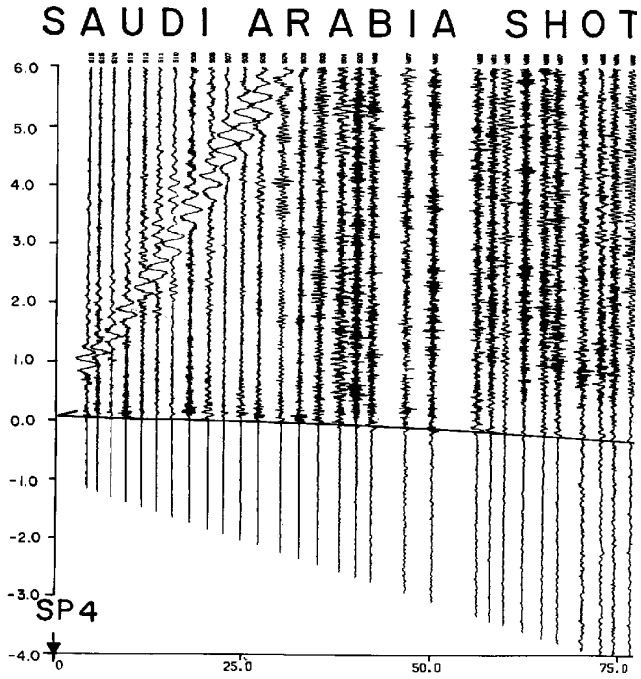

Fig. 11. Seismic record section for the data from shot point 4 NE. Presentation as in Fig. 6. Calc traveltimes are from the velocity model of Fig. 10d.

pp. 205–208

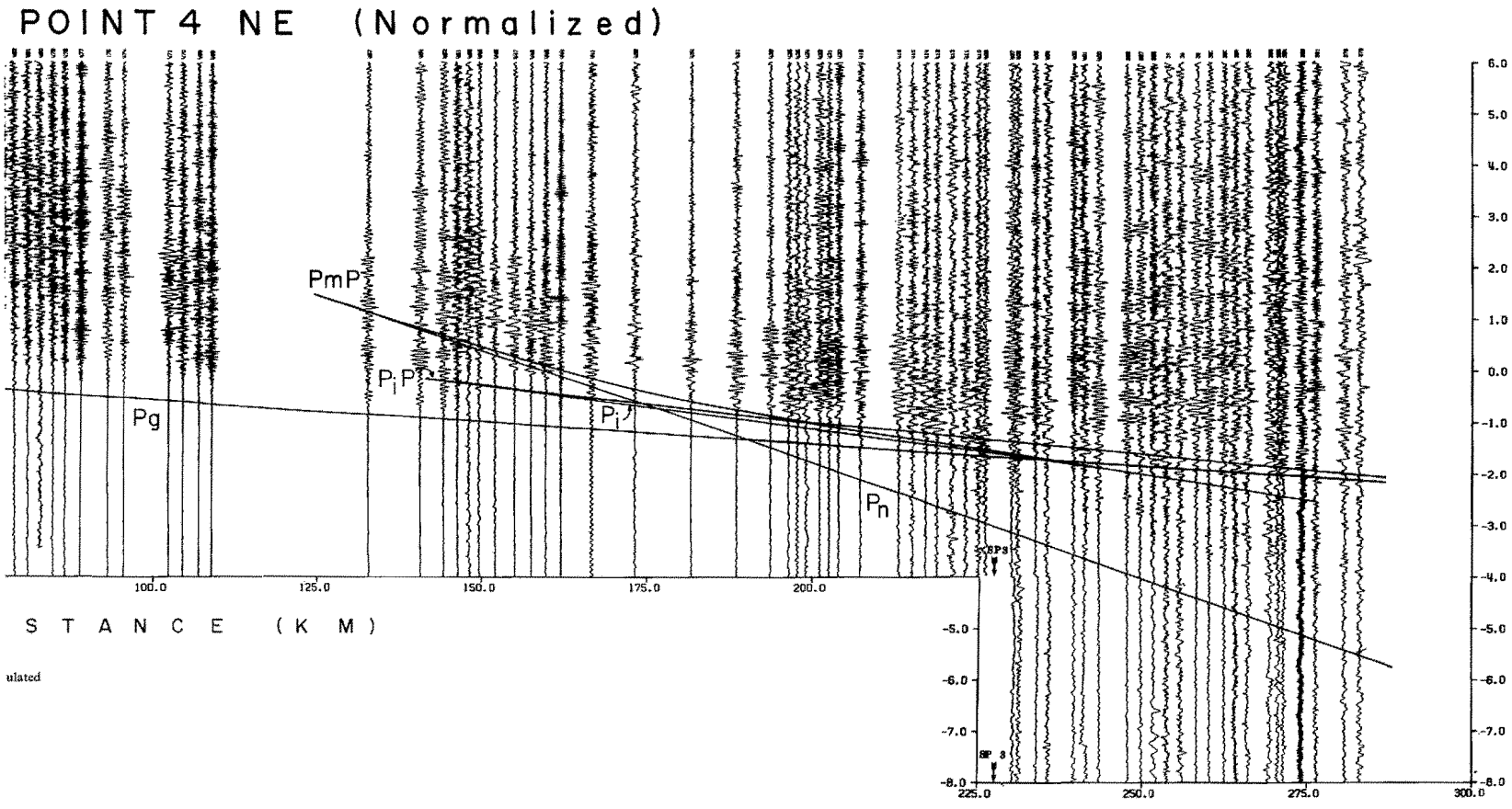

ulated

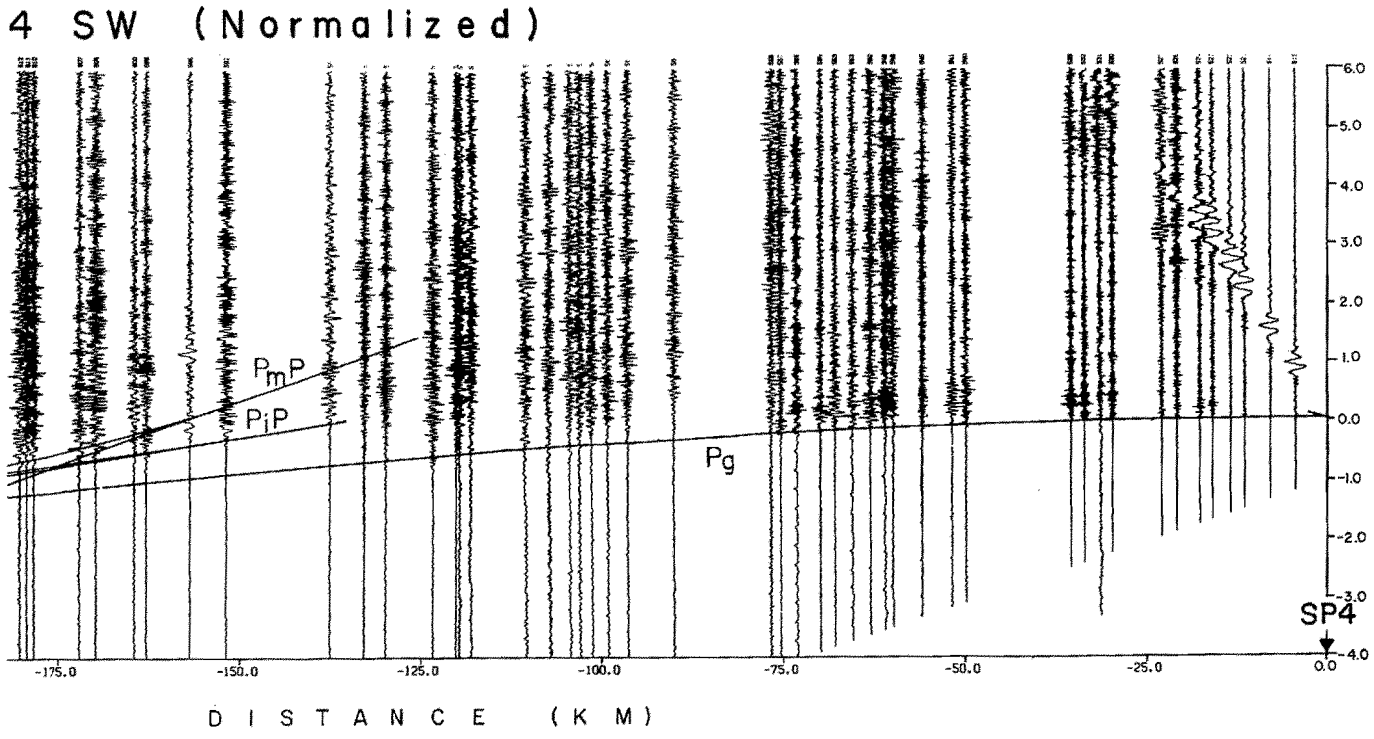
4 SW (Normalized)
PmP
PiP
Pg
SP4
6.0
5.0
4.0
3.0
2.0
1.0
0.0
-1.0
-2.0
-3.0
-4.0
-175.0
-150.0
-125.0
-100.0
-75.0
-50.0
-25.0
0.0
DISTANCE (KM)

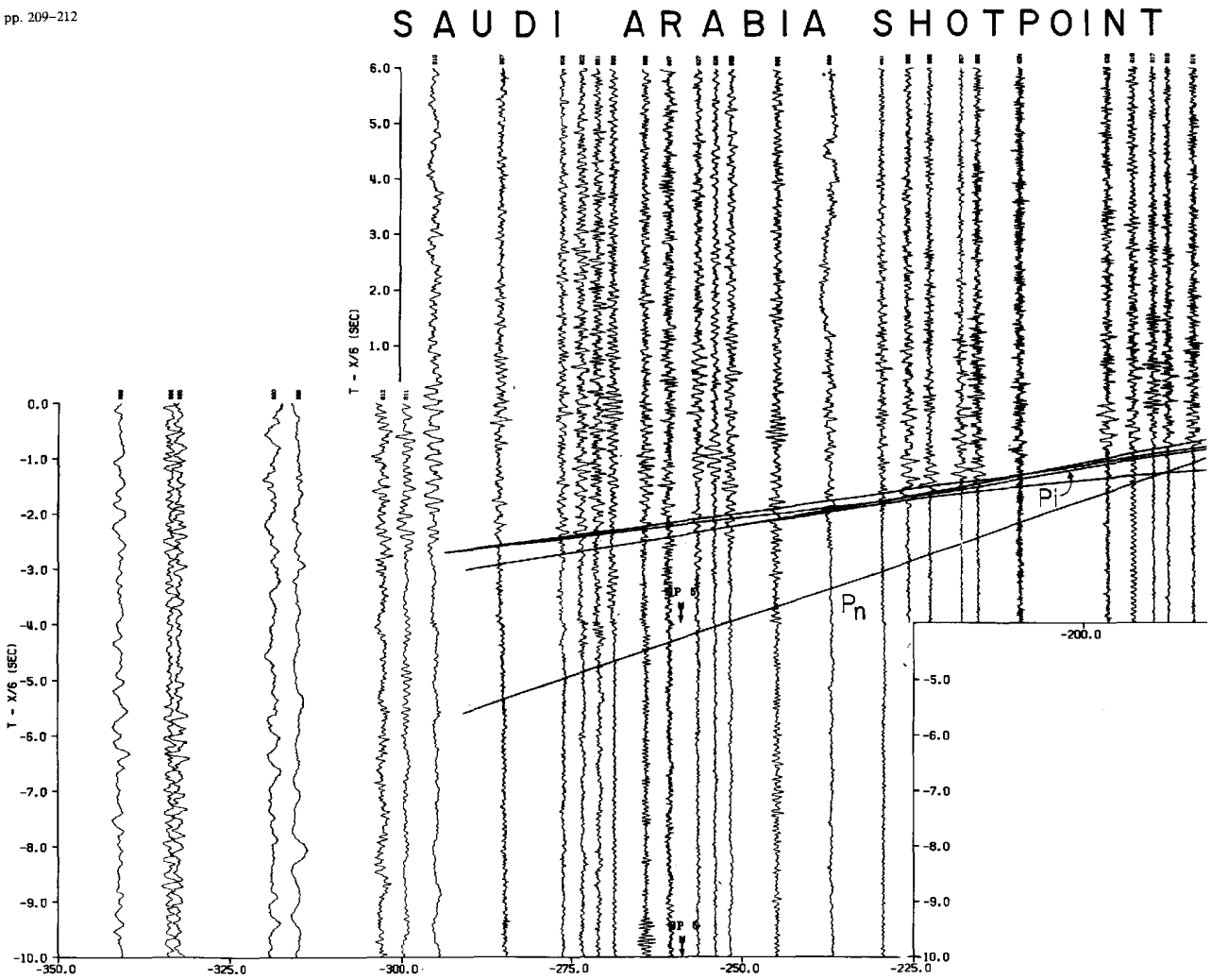

Fig. 12. Seismic record section for the data from shot point 4 SW. Presentation as in Fig. 6. Calculated traveltimes are from the velocity model in Fig. 10d.

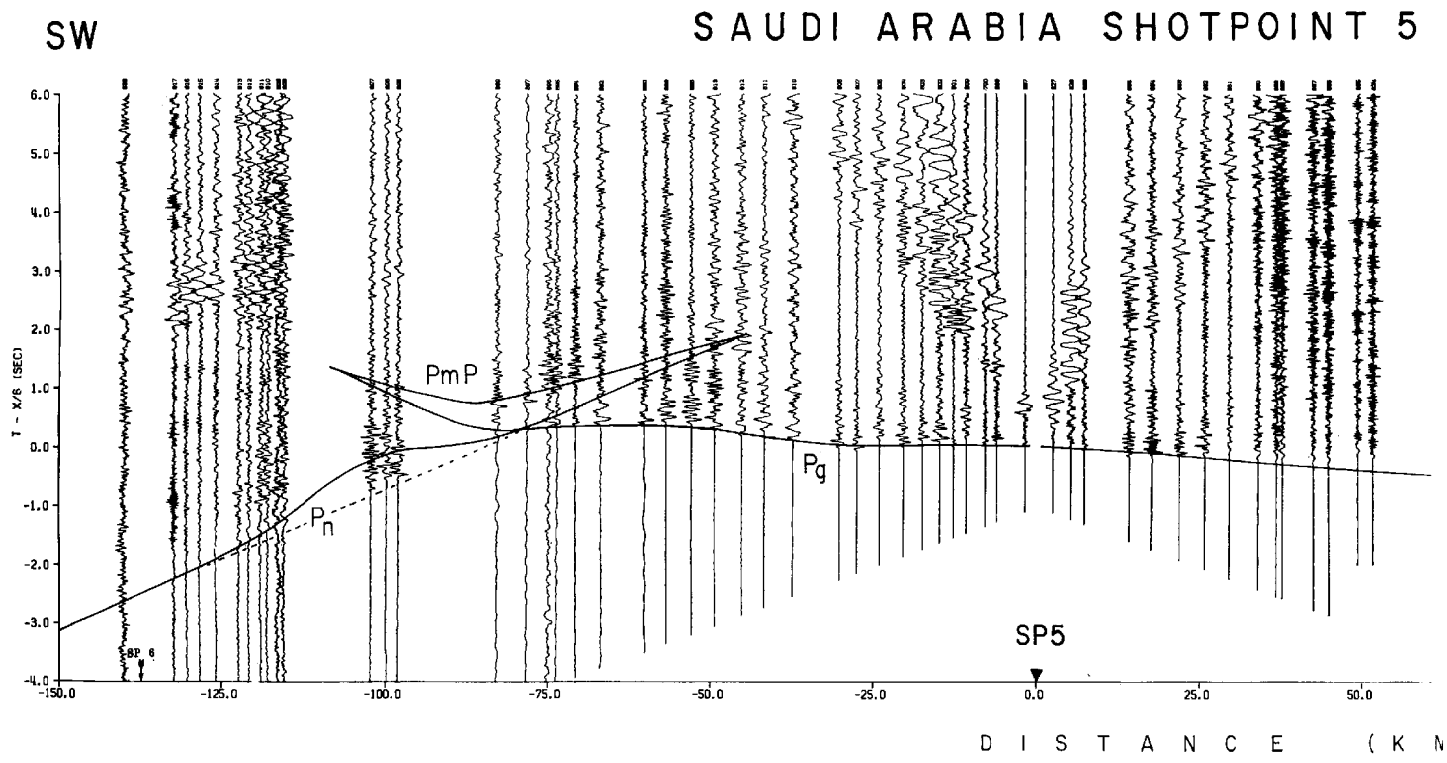

Fig. 13. Seismic record section for the data from shot points 5 NE and 5 SW. Presentation as in Fig. 6. Calculated traveltimes are from the velocity model in Figs. 10d and 14d.

(Normalized)

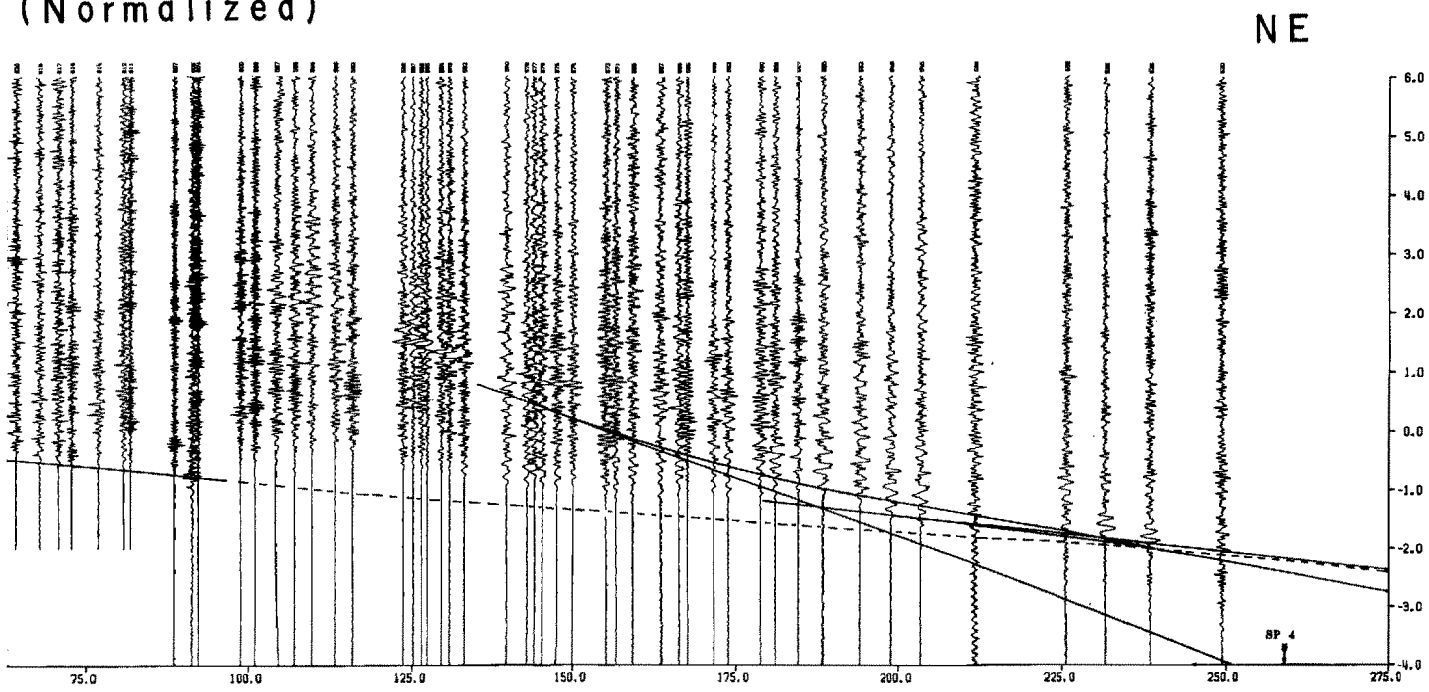
NE
6.0
5.0
4.0
3.0
2.0
1.0
0.0
-1.0
-2.0
-3.0
-4.0
SP 4
75.0
100.0
125.0
150.0
175.0
200.0
225.0
250.0
275.0

( )

pp. 218–222

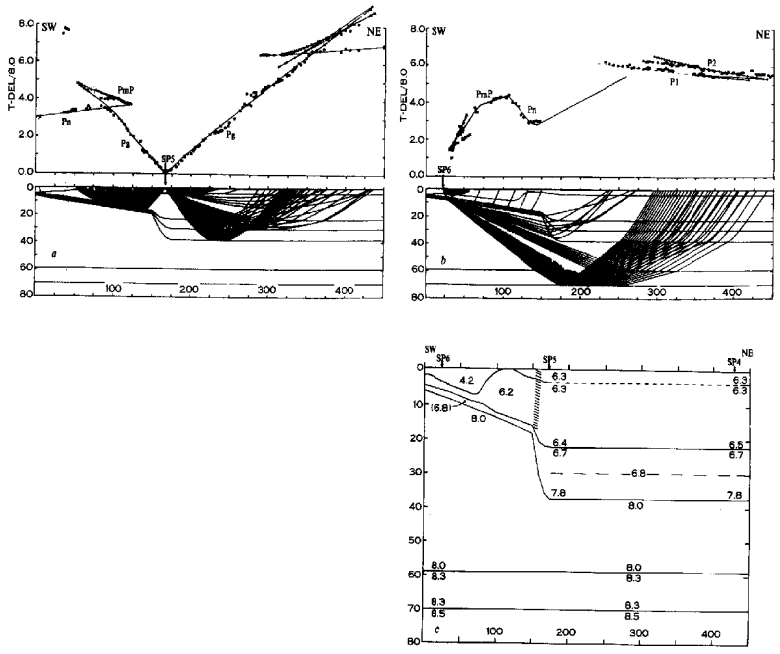

Fig. 14. Two-dimensional ray-trace models for the data from shot points 5 SW and 5 NE (a) and 6 NE (b). These data cross the Red Sea–Shield transition. Presentation as in Fig. 5. The velocity model is shown in panel (c).

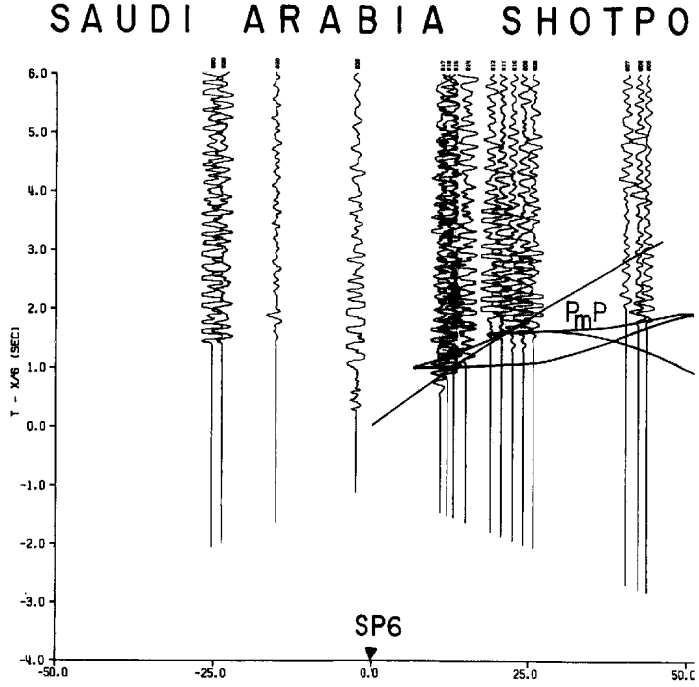

Fig. 15. Seismic record section for the data from shot point 6. Calculated traveltimes are from the velocity model of Fig. 14C. Presentation in Fig. 6.

INT 6 NE (Normalized)

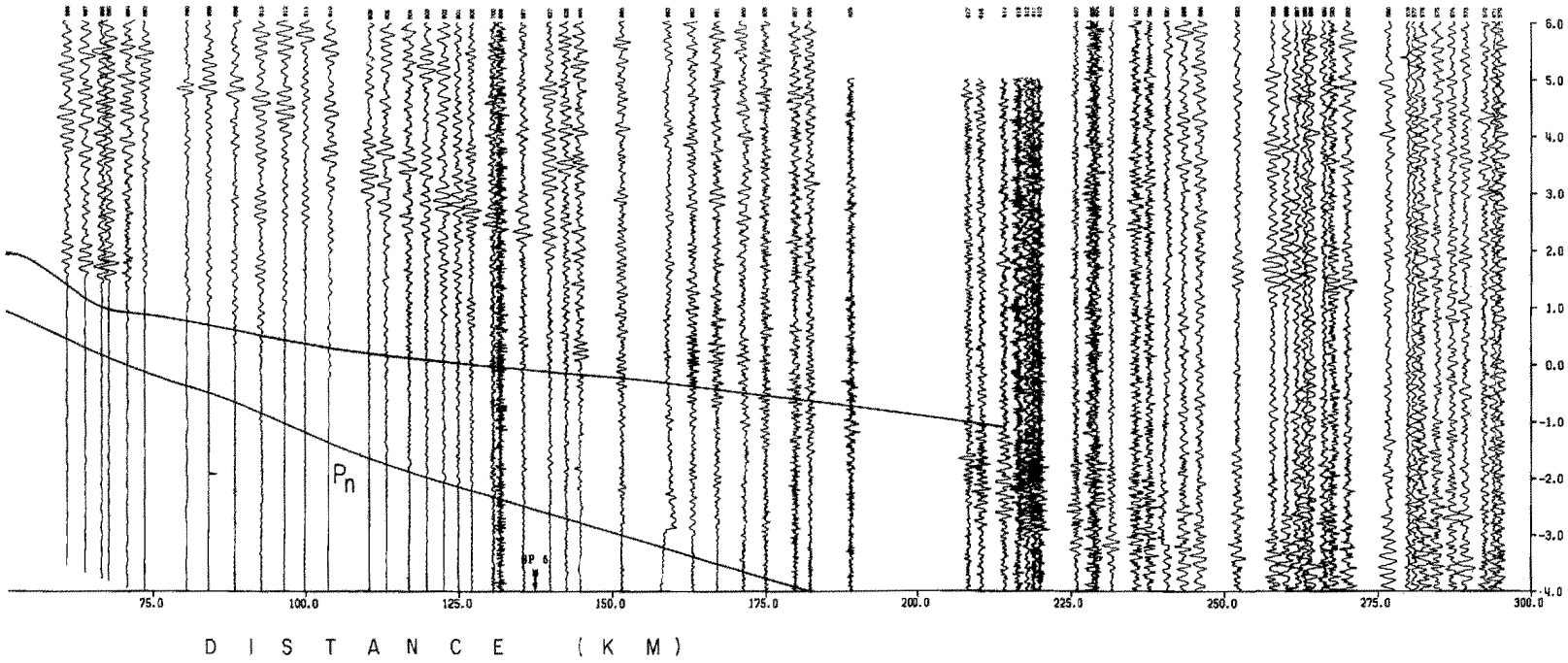

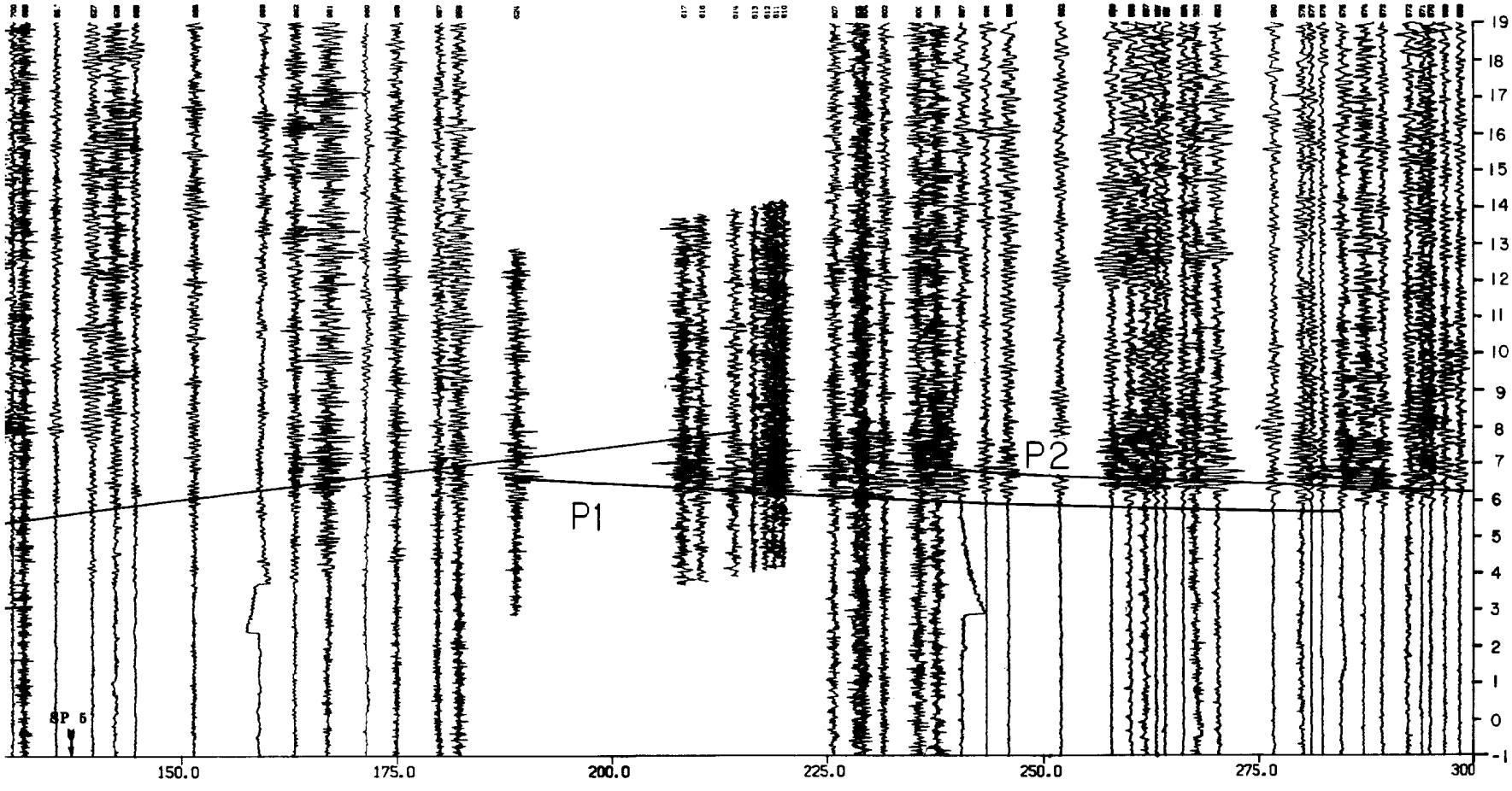
P1
P2
SP 6
150.0
175.0
200.0
225.0
250.0
275.0
300
19
18
17
16
15
14
13
12
11
10
9
8
7
6
5
4
3
2
1
0
-1

C E (K M)

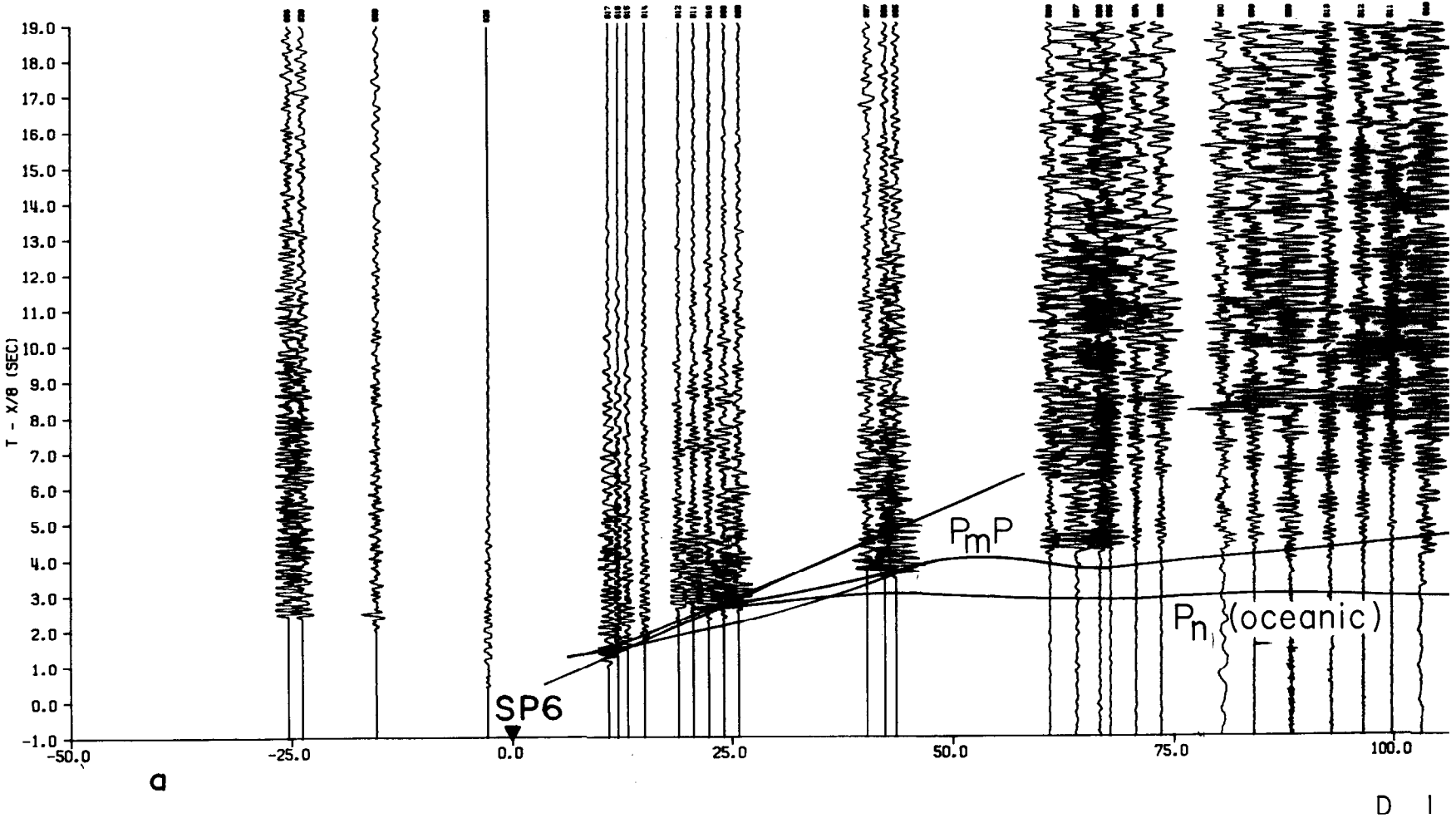
SAUDI ARABIA SHOTPOINT 6 NE (True Am
T - X/8 (SEC)
19.0
18.0
17.0
16.0
15.0
14.0
13.0
12.0
11.0
10.0
9.0
8.0
7.0
6.0
5.0
4.0
3.0
2.0
1.0
0.0
-1.0
-50.0
-25.0
0.0
25.0
50.0
75.0
100.0
SP6
PmP
Pn (oceanic)
a
D I

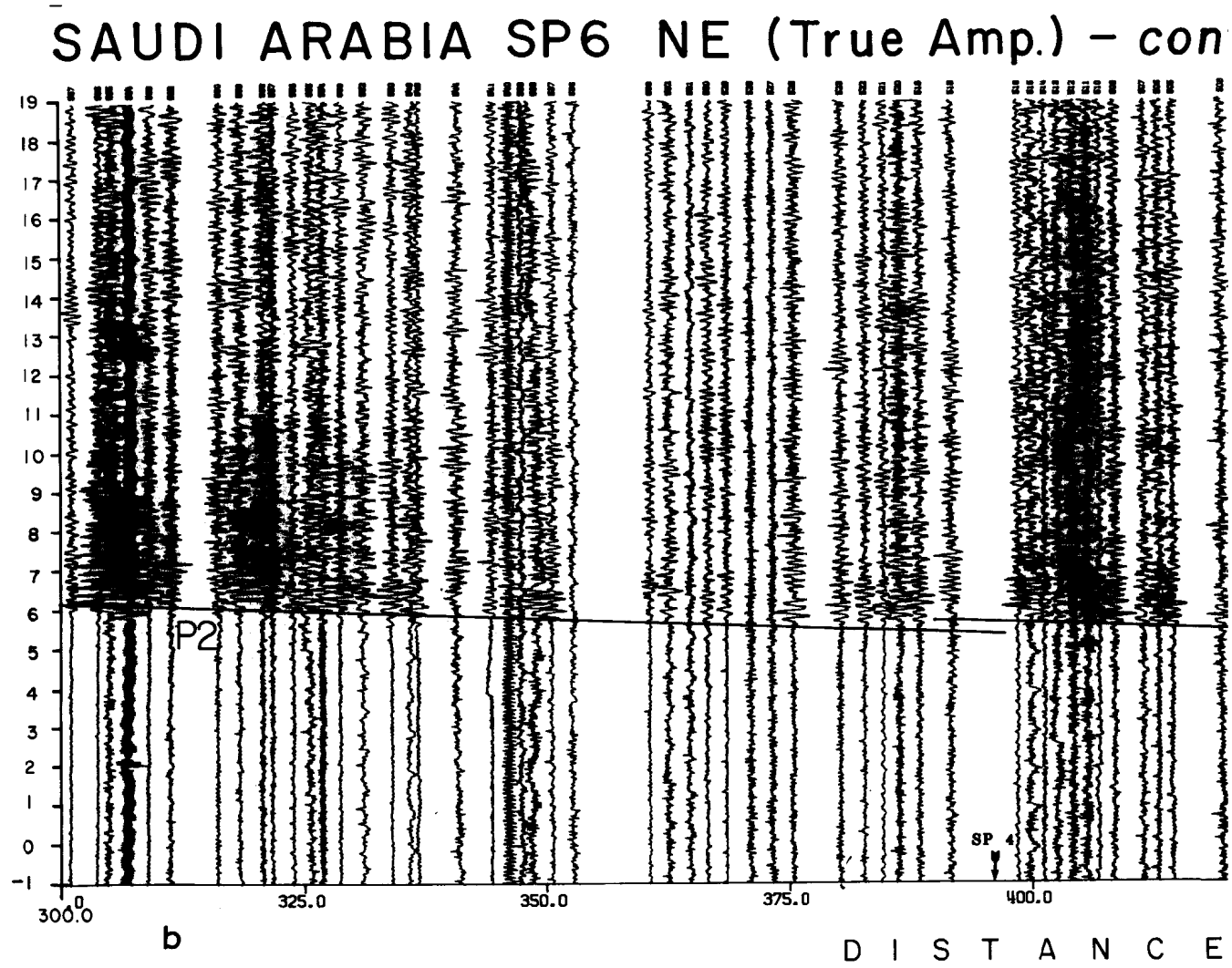

Fig. 16 (continued).

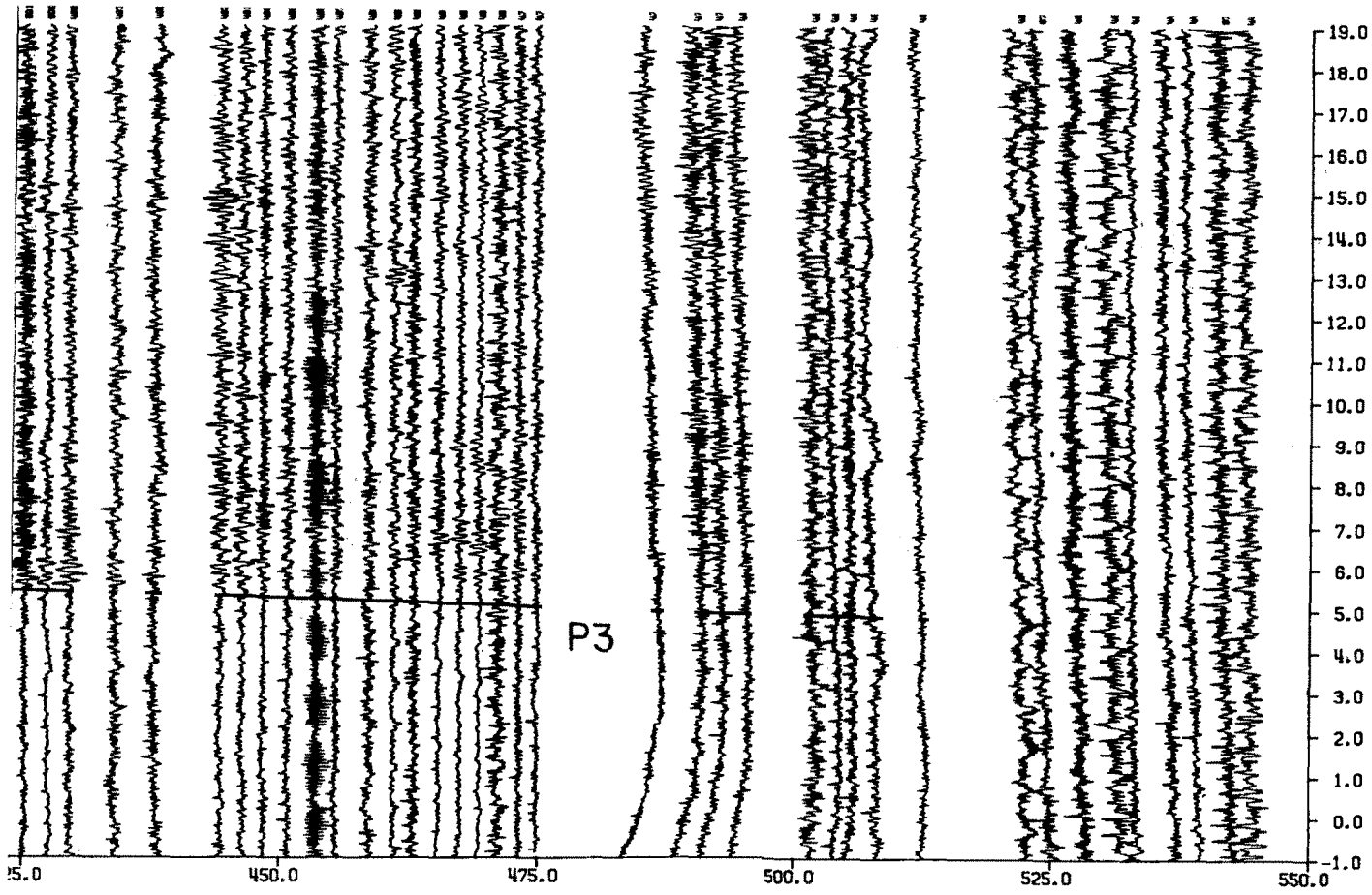
P3
19.0
18.0
17.0
16.0
15.0
14.0
13.0
12.0
11.0
10.0
9.0
8.0
7.0
6.0
5.0
4.0
3.0
2.0
1.0
0.0
-1.0
425.0
450.0
475.0
500.0
525.0
550.0
(K M)

probably upper crustal heterogeneities between shot points 1 and 2 that have not been resolved in the present modeling.

The two-dimensional model fits the P_mP and P_n phases for profile 1 SW reasonably closely, but it predicts a P_n phase where none is clearly visible from shot point 2 NE (Fig. 7). These difficulties in modeling the lower crust and upper mantle between shot points 1 and 2 suggest that strong lateral heterogeneity characterizes the entire region.

The modeled traveltimes reasonably fit all arrivals from shot point 2 SW (Figs. 5b, 8); this good fit is not unexpected because the model is very similar to the successful flat-layer model (Fig. 2d). The record section data (Fig. 8) shows very clear P_iP and P_mP arrivals between 125 and 225 km. Mantle refractions (P_n) are less clear than for those from shot point 1 SW (Fig. 6). The data from shot point 3 NE (the reverse of shot point 2 NE) provide only P_g arrivals (Fig. 9), and these indicate a near-surface velocity of about 6.0 km/s.

The average upper crustal velocity between shot points 1 and 3 is approximately 6.25 km/s and shows a variation of 0.2 km/s at a given depth. The mid-crustal discontinuity occurs at 21 km depth (Fig. 5d). For profile 2 SW there is a strong velocity gradient (from 6.8 to 7.9 km/s) in the lower crust between 31 and 43 km depth, and the velocity contrast at the M-discontinuity is only 0.2 km/s. The effect of the high lower crustal gradient is shown quite clearly in the ray-trace of Fig. 5b, where rays passing through the lower crust are focused between 128 and 160 km on the distance scale. Prodehl (1985, this volume) derives a similar model for the lower crust based on synthetic seismogram calculations.

In summary, strong lateral velocity variations are evident between shot points 1 and 2. Southwest of shot point 2 there is a region of refraction overlap (both profiles 1 SW and 2 SW extend into it) but not of refraction reversal. The differences in crustal structure northeast and southwest of shot point 2 seem resolvable; we suggest (Fig. 5b) that a major crustal boundary occurs near the shot point.

Shot points 5–4–3

The profile sets for shot points 3, 4, and 5 (Figs. 9–13) cover the southwestern portion of the Najd tectonic province and all of the Hijaz-Asir tectonic province and cross several major crustal features including the Nabitah zone, the Al Qarah gneiss dome, and the Hijaz-Asir escarpment.

The arrivals through the basement (P_g) have been reasonably well fit for the four profiles considered here, except for the data from profile 5 NE across the Khamis Mushayt gneiss (Fig. 13). The high upper crustal velocity in that area was discussed in the section on flat-layer models. For profile 3 SW the composite model (Fig. 10) gives reasonably good traveltime fits for both the P_iP and the P_mP reflection (Fig. 9). Traveltimes of the composite velocity model fit the P_n arrivals quite well.

In discussing the data of profiles 4 NE and SW (Figs. 11, 12), we reemphasize a previously made observation: the seismograms on these profiles have a high domi-

nant frequency coda that makes phase correlation of secondary arrivals very difficult. Therefore, we have given greater weight to the traveltime models of profiles 5 NE and 3 SW in constructing the composite model.

The agreement between the visible secondary arrivals and those calculated for the composite model is good despite the difficulty in identifying secondary arrivals in the data from shot point 4 (Figs. 11, 12). However, the composite model does not account for the prominent secondary arrivals following P_g, about 80 km northeast of shot point 4. (These arrivals, calculated to be caused by a reflector at 13 km depth, are included in the interpretive section, Fig. 17).

P_n arrivals are poorly observed in the data for either profile 4 NE or 4 SW. In profile 4 SW, the mid-crustal reflector at 22 km appears to fit observed P_iP arrivals reasonably well (Fig. 12). P_mP arrivals are not clear; in fact, most secondary arrivals can be explained by the P_i–P_iP curves alone. The theoretical P_iP and P_mP curves nearly merge beyond 185 km.

The composite velocity model fits the data of profile 5 NE reasonably well (Fig. 13). We have already discussed the high-velocity upper crust in the vicinity of the Khamis Mushayt gneiss; this abrupt traveltime advance has been accurately modeled and the high velocity has been included in the interpretive section (Fig. 17). The good fit of ray-trace model for the mantle reflection (P_mP) and refraction (P_n) indicates that the average crustal velocity and thickness of the model are consistent with the data.

In summary, the velocity model for profile sets 3, 4, and 5 is adequately represented in Fig. 10d. The prominent high-velocity region between shot points 4 and 5 corresponds to the Khamis Mushayt gneiss. The crust is 40 km thick, with high velocities (6.8–7.8 km/s) in the lowermost crust. There is also evidence for a 13-km-deep reflector between shot points 3 and 4, which is not shown in Fig. 10d but is included in Fig. 17.

Shot points 6–5

The region between shot points 5 and 6 spans the Red Sea–Shield transition zone at the southwestern end of the profile (Fig. 1). Shot point 5 is about 5 km to the northeast of the dike swarms of the Tihamat Asir, which are believed to be at the margin of the Red Sea rift. Southwest of shot point 5 are the coastal plain and Red Sea shelf sediments, which have been drilled to 4 km depth in the offshore regions (Gillmann, 1968).

Our discussion begins with profile 6 NE (Figs. 14b, 15, 16), which was not discussed in the section of flat-layer modeling. The two ray-trace diagrams of Fig. 14 are for traveltimes reduced by 8.0 km/s, unlike the previous figures. The record section for shot point 6 is displayed with reduction velocities of both 6.0 km/s (Fig. 15) and 8.0 km/s (Fig. 16). The pattern of arrivals is extremely irregular; the only certain correlations are crustal arrivals between 1 and 26 km and P_n arrivals between 105 and 125 km. Between 26 and 105 km distance, the data show a series of

traveltime advances and delays that may result partly from large variations in the thickness of low velocity sediments. Between 18 and 27 km, high-amplitude secondary arrivals follow the first arrival by 0.4 to 0.15 s. We interpret these secondary arrivals as mantle reflections (P_mP). According to this correlation, the depth to the mantle 22 km east of shot point 6 is 8 km. However, if the P_mP critical point at 22 km is connected with a straight line to the clear P_n arrivals at 105 km, the line is approximately 1.0–1.5 s ahead of the visible first arrivals. Two possible explanations exist for this. The first is that the velocity structure varies strongly laterally between 26 and 105 km, and large traveltime delays occur in that range because of the thickening of sedimentary rocks. The second possible explanation is that the visible first arrivals are actually secondary arrivals and the mantle refraction is of extremely low amplitude (resulting perhaps, from irregular structure at the crust–mantle interface). The record section (Fig. 15) indicates possible very weak earlier arrivals between 58 and 105 km.

Regardless of these uncertainties, a relatively simple model was derived by connecting the 8-km-thick crust at shot point 6 to the 17.5-km-thick crust southwest of shot point 5 (the latter is the midpoint of the velocity gradient derived in flat-layer modeling, see Fig. 4b). We used iterative two-dimensional ray-tracing to somewhat refine the initial model. The model fits the P_g arrivals and the mantle refractions (P_n) in the traveltime data of profile 5 SW (Fig. 13) reasonably well, but mantle refraction arrivals (P_n) appear to be delayed by as much as 1.0 s at 100 km.

For profile 6 NE (Fig. 15), the arrivals at 0–45 km and P_n at 105–125 km are fit rather well by the ray-trace calculations. The detailed traveltime behavior of arrivals between 60 and 100 km is not well fit.

In summary, the data from profiles 5 SW and 6 NE have been interpreted to indicate a landward dip of the M-discontinuity of 4.6°. The P_n velocity is 8.0 km/s, and the crust consists of a 4.2-km/s layer on top of a thicker 6.2–km/s layer. More densely recorded data would be desirable to further reveal the structure in this important tectonic region.

In the region of the Arabian Shield–Red Sea transition, the especially weak and diffuse arrivals between 150 and 200 km from shot point 6 (Fig. 16a) probably indicate extreme structural complications. Beyond this structural transition, the strong arrivals observed, which begin about 225 km from the shot point, show an en echelon pattern of first and secondary arrivals; the secondary arrivals have high amplitudes at distances of 225, 325, and 400 km (Fig. 16a, b). Previously conducted long-range refraction profiles have determined that these phases indicate velocity gradients or discontinuities in the upper mantle (e.g., Hirn et al., 1973; Kosminskaya et al., 1972). We have attempted to model only two of the en echelon mantle phases (labelled P_1 and P_2 in Fig. 14b) and show them as first-order discontinuities at depths of 59 and 70 km, where the velocity increases from 8.0 to 8.3 km/s and from 8.3 to 8.5 km/s, respectively.

It is of some interest to note in the ray-trace diagram (Fig. 14b) that from shot

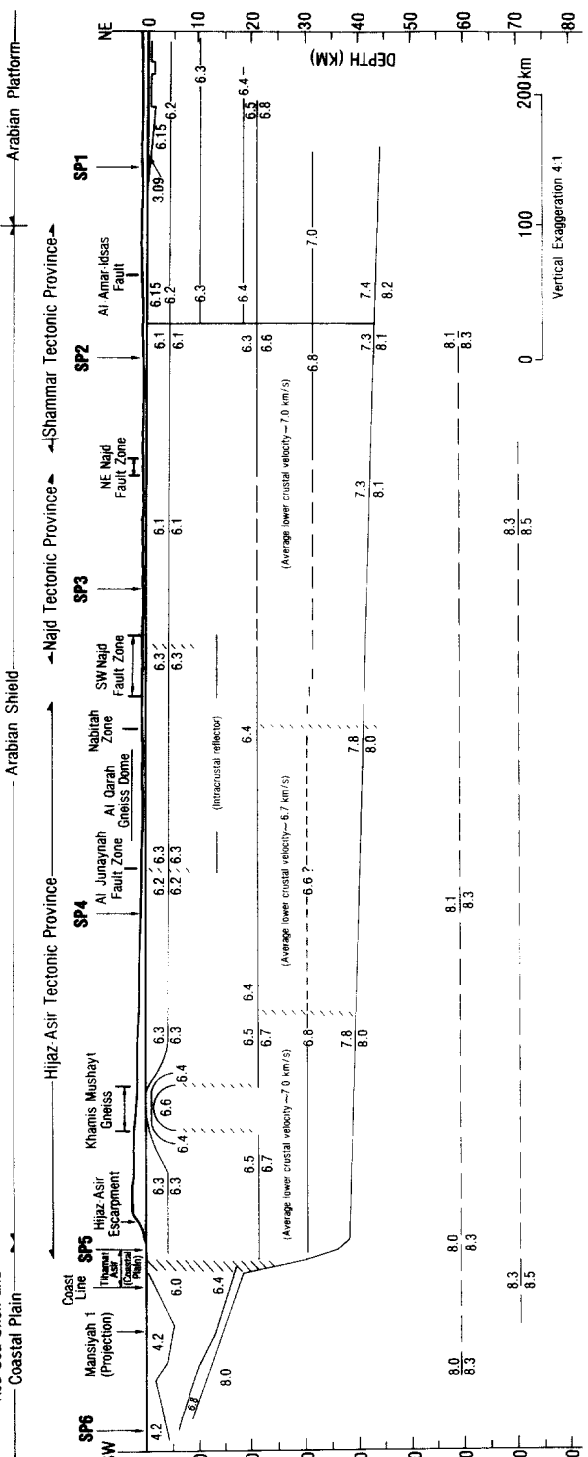

Fig. 17. Composite cross section of the crust and upper mantle of the Arabian Shield from the Red Sea to the Arabian Platform. The major features are discussed in the text.

point 6 there is no true P_n phase, that is, no head or diving waves traveling along the continental M-discontinuity, beneath the Shield. This observation raises the possibility that similar phases modeled in previous offshore-onshore investigations as head waves are, in fact, reflected upper mantle phases.

The two-dimensional velocity models have been combined into the interpretive section of Fig. 17. Its major features are outlined in the Discussion section.

OTHER INTERPRETATIONS

The third triannual meeting of the International Association of Seismology and Physics of the Earth's Interior (IASPEI), Commission on Controlled Source Seismology (CCSS), convened in Park City, Utah, on August 11–17, 1980. Several days were devoted to a discussion of interpretations of the 1978 Saudi Arabia seismic deep-refraction data (Mooney, 1980). The complete refraction data set had been distributed to the fifty participants before the meeting to give each seismologist or team of seismologists time to analyze the data.

The participants' interpretations of the crustal and upper mantle velocity-depth structure beneath shot point 3 have been compiled for comparison and to illustrate the range of models permitted by the data (Fig. 18). The velocity–depth functions

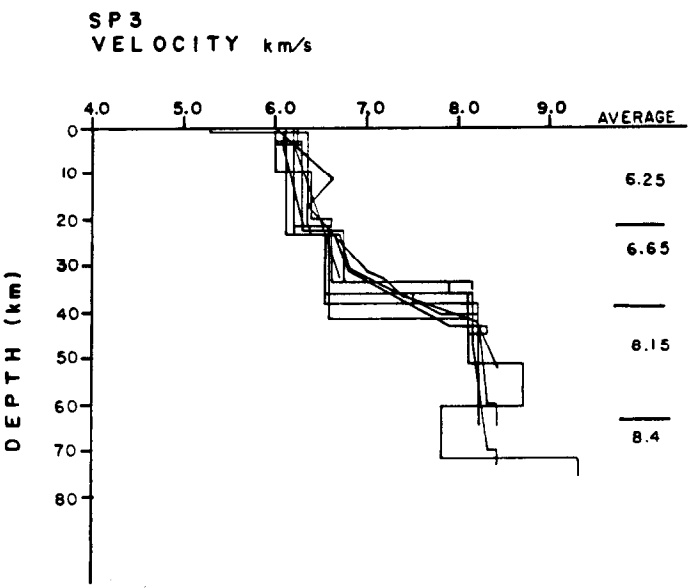

Fig. 18. Compilation of velocity–depth functions beneath shot point 3 as presented by the participants of the 1980 IASPEI—Commission on Controlled Source Seismology (CCSS) meeting (see text). Individual interpretations are indicated by solid lines, and the average structure is indicated to the right of the set of curves.

indicate an average upper crustal velocity of 6.25 km/s, and most interpretations place the mid-crustal boundary at around 20 km depth, with the average lower crustal velocity about 6.6–6.7 km/s. The velocity structures are of two basic types, those with homogeneous layers and those with velocity gradients within the layers. In discussion it was generally agreed that velocity gradients probably do exist within the crust and upper mantle. Some scatter is seen in the interpreted depths to the M-discontinuity, with the average depth being 39 km. In the upper mantle, it was generally agreed that the velocity increases between 40 and 60 km depth, either gradually or discontinuously. On the basis of long-range data from shot points 1 and 6 (Figs. 6 and 16) two interpretations show velocity discontinuities at 70 km depth; one of the models shows a pronounced low-velocity zone between 60 and 70 km depth.

To summarize, the CCSS workshop interpretation of the Saudi Arabian seismic deep-refraction data showed the following (Mooney and Prodehl, 1984):

(1) The upper crust of the Shield is 20–21 km thick and has an average velocity of about 6.3 km/s. In some regions there may be small velocity discontinuities and (or) low-velocity zones.

(2) The lower crust of the Shield is 18–19 km thick and is separated from the upper crust by a seismic discontinuity at which the velocity increases by about 3.0–0.4 km/s. The average velocity of the lower crust in the workshop interpretations is about 6.7 km/s; however, velocities greater than 7.0 km/s may be present in the lowermost crust. (In the present interpretation, the average velocity is 7.0 due to a high vertical velocity gradient in the lowermost crust.)

(3) The M-discontinuity is probably a 2–5-km-thick transition zone at a depth near 40 km. Uppermost mantle velocities appear to increase laterally from 8.0 km/s beneath the Red Sea to 8.2 km/s beneath the Arabian Platform.

(4) Considerable evidence exists for fine structure in the upper mantle between 40 and 70 km depth, including velocity discontinuities.

(5) The detailed structure of the crust and upper mantle is difficult to resolve between shot points 5 and 6, the Arabian Shield–Red Sea transition zone. Models derived by using the available data show a change in crustal thickness from 40 km on the Shield to 12 km in the Red Sea and considerable upper mantle structure.

Participants at the CCSS meeting recommended the following methods for future seismic refraction and reflection work at the ocean–continent transition in western Saudi Arabia:

(1) Parallel-to-structure refraction profiles, located along the coastal plain and in the Red Sea.

(2) Perpendicular-to-structure profiles, which must be densely recorded and include considerable data redundancy.

(3) Seismic reflection profiles, which would help resolve details in the areas of greatest structural complexity. Reflection profiles across the Hijaz-Asir escarpment would shed light on the structure of this rift boundary.

DISCUSSION

General seismic features of the Arabian Shield

First-order seismic structure of the Shield

To a first-order approximation, the Arabian Shield consists of two crustal layers (Fig. 17). The upper crustal layer is 20–21 km thick and has an average velocity of 6.3 km/s. The lower crustal layer is 18–19 km thick and has an average velocity of approximately 7.0 km/s. These two layers are separated by a midcrustal first-order velocity discontinuity, at which the velocity increases from 6.4 to 6.7 km/s. The crust–mantle discontinuity may be marked by a velocity increase of only 0.2–0.4 km/s due to the high velocity gradient in the lowermost crust. The crustal thickness increases from about 38 km beneath the Red Sea to about 43 km beneath the Arabian Platform. The Red Sea–Shield transition is marked by a change in crustal thickness from less than 20 km to 38 km, over a distance of about 25 km. Beneath the sedimentary section of the Tihamat Asir coastal plain and Red Sea shelf, the average crustal velocity is 6.2 km/s.

Although this first-order model fits the average traveltimes of the record sections, significant deviations from predicted arrival times and varying frequency content and amplitude of individual seismograms indicate lateral inhomogeneities within the crust. Detailed comparison of the geologic sections with the record sections show considerable correlation between velocity variations and lithologic and structural features; we proceed in our discussion from northeast to southwest.

Some second-order structures of the Shield

(1) We have identified a lateral boundary in the upper crust 30 km northeast of shot point 2 across which velocities increase to the northeast by about 0.2 km/s (Fig. 17). These relatively high upper crustal velocities (6.3–6.5 km/s) may be attributed to the higher metamorphic grade of these rocks, and the velocity change indicates that the crust here is different from that to the west, as suggested by Schmidt et al. (1979). Northeast of the boundary, the lower crustal velocities below a depth of 30 km have appear to a lower gradient than those along other parts of the profile, and the mantle velocities are higher than those along other parts of the profile. The boundary zone, as seismically determined, is about 40 km southwest (along the profile) of the Al Amar–Idsas fault, which has been commonly accepted (Schmidt et al., 1979) as marking the western edge of an allochthonous continental block. On the basis of the seismic evidence, uncertainty as to the location of the boundary is about ± 15 km; therefore, the boundary is at least 25 km southeast (along the profile) of the Al Amar–Idsas fault. Delfour (1979) suggested that the Abt schist, which extends from the Al Amar–Idsas fault southwest to the seismic boundary, may contain unidentified thrust faults; an imbricate structure for the Precambrian collision zone (Schmidt et al., 1979) would explain the displacement of the seismi-

cally determined zone from the Al Amar–Idsas fault. Because the refraction data at this level of interpretation cannot resolve the dip of the zone or even its direction, we have drawn it vertically in Fig. 17, as we have drawn all other zones between laterally inhomogeneous parts of the crust.

(2) We cannot distinguish the southwestern part of the Shammar tectonic province from the Najd province (Fig. 17) at this level of seismic interpretation because of the lack of data along profile 3 NE; the crustal structure is undoubtedly more complicated than Fig. 17 represents. The velocities observed are typical of those in crystalline upper crustal rocks. However, the lower crustal velocities (20–40 km depth) are anomalously high and atypical of granitic crust; they are more indicative of mafic crust. The evolutionary models of Schmidt et al. (1979) involve crustal formation from collisions of island-arc systems.

At the southwest Najd fault zone, which delimits the southwestern boundary of the Najd tectonic province (between 35 and 80 km southwest of shot point 3), there is a lateral seismic discontinuity across which uppermost crustal velocities increase from 6.1 km/s in the northeast to 6.3 km/s in the southwest (Fig. 17). The high-velocity region apparently includes the fault zone. In addition, we interpret an intracrustal reflector beneath the fault zone at about 13 km depth. This reflector correlates well with gravity anomaly highs and large magnetic signatures (Gettings et al., 1983). Estimates of the center of mass of the gravity anomaly yield depths of 15–20 km, and we infer that the reflector marks the top of the source. We interpret the reflector as mafic intrusions into the fault zone at upper crustal levels.

(3) We observed a lateral velocity discontinuity in the uppermost crust in the vicinity of shot point 4, at the Al Junaynah fault zone. Southwest of the fault zone, velocities are lower, about 6.2 km/s, for about a distance of 60 km. They then increase dramatically toward the Khamis Mushayt gneiss (Coleman, 1973) and reach 6.6 km/s at depths of only 5 km in the core of the gneiss. This high-velocity region correlates closely with the outcrop pattern of the Khamis Mushayt gneiss and appears to penetrate the entire upper crust. It is the best example along the profile of the geophysical expression of a dome, in which lower crustal material has been brought to the present-day surface.

Western Shield margin and the Red Sea rift and shelf

The most dramatic crustal and upper mantle transition along the profile is that from the westernmost Shield to the Red Sea rift and shelf. The velocity structure of the Shield directly beneath shot point 5 is roughly the same as that throughout the Shield (Fig. 17), and the transition to the thin crust of the shelf occurs over only 25 km distance southwest from shot point 5. The change in crustal thickness here is as abrupt as anywhere in the world. The seismically determined transition coincides at the surface of the Tihamat Asir with a sharp boundary between the Precambrian rocks and the Tertiary volcanic and intrusive rocks (Fig. 17).

A simple three-layer crust composed of sediments (4.2 km/s), an upper crust (about 6.2 km/s), and a thin lower crust (6.8 km/s) characterizes the Red Sea shelf and rift. The crust thins from 18.0 km at the coast to 8 km at shot point 6. Mantle velocity is 8.0 km/s.

In our seismic interpretation, we have presented a continental crust of "normal" thickness and velocity structure beneath the Arabian Shield, a crust of "transitional" thickness and velocity structure southwest of the Shield margin, and a crust of "normal" oceanic thickness and "transitional" velocity beneath the Red Sea shelf. The crust southwest of the Shield margin (shot point 5) is probably about 18 ± 4 km thick; because it has an average velocity of about 6.1 km/s, and diabase is the chief component where basement is exposed, it probably consists mainly of diabase. This velocity is intermediate between the velocities of Layers 2 and 3, typical of ocean basins (cf. Drake and Girdler, 1964); however, the seismic data do not allow us to discriminate between diabase, a mixture of Layers 2 and 3, and a typical sialic crust. This 6.1-km/s crust apparently passes westward into crust of "normal" oceanic thickness underlying the outer Red Sea shelf; the hypothesis that this is oceanic crust is strengthened by the fact that the 6.1-km/s crust beneath the Miocene sediments is only about 4 km thick, which seems much too thin to have resulted from attenuation of continental crust.

Lower crustal structure

At this stage of the interpretation, the evidence for lateral change in the velocity structure in the lowermost crust is primarily based on somewhat subjective judgments as to the amplitude behavior of the P_mP traveltime curve. A smaller velocity gradient in the lower crust and a correspondingly larger velocity contrast at the M-discontinuity was used to model those record sections that show the P_mP curve beginning at the shortest distance and spread over the largest range. By contrast, a higher velocity gradient causes the energy in the P_mP traveltime curve to be focused in a narrow range. For example, compare the behavior of the rays for shot point 2 NE (not focused) with that for 2 SW (focused) (Fig. 5b). In Fig. 17, the higher gradients in the lower crust are to the southwest of the Nabitah zone and the lower gradients are to the northeast. The M-discontinuity is sharp beneath the Red Sea shelf and has a velocity contrast of 1.2 km/s.

Isostasy and Moho structure

Upper mantle velocities at the M-discontinuity vary from 8.0 km/s between shot points 6 and 3 to 8.1–8.2 km/s between shot points 3 and 1. The velocity–depth structure of the upper mantle is presented as being uniform along the length of the profile; we see a first order discontinuity at a depth of 60 km, with a velocity increase from 8.0–8.1 to 8.3 km/s, and another at a depth of 70 km, with an increase from 8.3 to 8.5 km/s (Fig. 17).

In our model, the thickness of the crust, as defined by the depth to the M-discontinuity, increases northeastward from about 8 km near the Red Sea axis to 18 km beneath the shelf and coastal plain, increasing abruptly to 38 km beneath the western margin of the Shield, and then gradually to 43 km beneath the Arabian Platform. Most of the interpretations by CCSS participants show roughly the same relationships, except that several have a zone of thickened crust (to a depth of about 42 km) in the area of shot point 4 and westward (Mooney and Prodehl, 1984).

None of the interpretations given at the 1980 IASPEI–CCSS meeting indicate that the thickest crust coincides with the area of greatest topographic relief; models that feature a thickened crust between shot points 5 and 4 all show the thickest crust displaced by varying distances (up to 200 km) to the east of the topographic maximum. This feature implies a less dense upper mantle toward the southwest, at least from shot point 4 onward, if isostatic equilibrium is to be maintained (Gettings et al., 1983).

The more mafic character of the crust northwest from the Nabitah suture zone (Schmidt et al., 1979) somewhat, but not completely, offsets the need for a less dense upper mantle. The seismic observations are in agreement with the peculiar shape of the regional gravity profile described above. The gravity relations, as constrained by seismic refraction and geologic considerations, require both a more dense crust and a less dense upper mantle southwest of the Nabitah zone (Gettings et al., 1983).

Comparison of the crustal velocity structure of Saudi Arabia with those of other regions

We compare the crustal velocity structure of the Arabian Shield with those of other shields and platforms and other geologic provinces of similar crustal thickness to determine what features are held in common. The Arabian Shield shares many characteristics with the Ukranian and Baltic Shields and the Turanian and Russian Platforms (Fig. 19; Kosminskaya et al., 1969; Sollogub, 1969). The thickness of the upper crust in those regions is 20 ± 5 km, and the average velocity below the sediments is 6.2 km/s; the mean crustal thickness is 40 km, and the average lower crustal velocity is 7.0 km/s. These values are remarkably similar to those determined for the Arabian Shield (Fig. 19).

Mykkeltveit's (1980) interpretation of the crustal structure of the Fennoscandian Shield (Norway) is also quite similar to that for Saudi Arabia. The upper crust is 19.5 km thick and has an average velocity of 6.2 km/s. The average velocity of the lower crust is 6.8 km/s, and the total crustal thickness is 40 km. Mykkeltveit also shows details in the structure of the Fennoscandian Shield, including a low-velocity zone, that correlate with features in the interpretation of Prodehl (1984), although they do not appear in our average sections of Fig. 19.

The western Canadian Shield (Hall and Hajnal, 1973) appears to have an upper crustal velocity (6.05 km/s) lower than that of the Arabian Shield, but a similar lower crustal velocity (average 7.0 km/s). The thickness of the upper crust is 19 km,

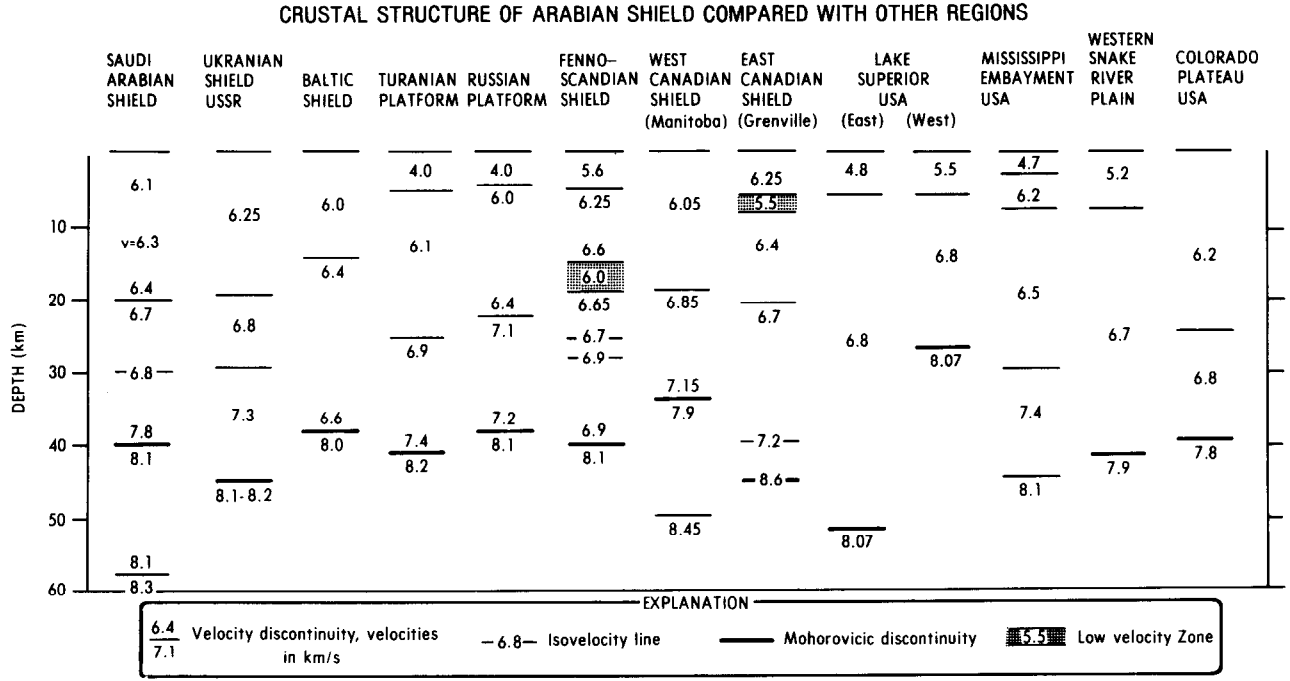

Fig. 19. Seismically determined crustal structure of the Arabian Shield compared with those of other regions. Velocity gradients are indicated by two or more velocities between a set of solid lines. References in text.

similar to that of the Arabian Shield, but the lower crust is about 5 km thinner, for a total crustal thickness of only 34 km; the western Canadian Shield appears to be anomalously thin compared to the Arabian Shield and other shields and platforms.

In contrast, the Grenville province of the northeastern Canadian Shield shows a crustal thickness of about 43 km; the M-discontinuity is modeled as a gradient at 40–45 km depth across which the velocity increases from 7.2 to 8.6 km/s (Berry and Fuchs, 1973). The lower crust above the M-discontinuity is approximately the same thickness and has about the same average velocity as the Arabian Shield. The upper crust also has a similar average velocity and thickness as compared to the Arabian Shield; moreover, upper crustal low-velocity zones are marked similarity to those in some of the 1980 IASPEI–CCSS interpretations (Mooney and Prodehl, 1983).

The crust of the Arabian Shield is very different from some of the well-studied interior regions of the United States and Canada. Although Lake Superior (Smith et al., 1966), the Mississippi embayment (McCamy and Meyer, 1966; Mooney et al., 1983), and the western Snake River Plain (Hill and Pakiser, 1966) all have comparable crustal thicknesses, they have high velocities at depths as shallow as 6 km, that is, 14 km shallower than the depths determined for the Arabian Shield. One interpretation of the shallow high-velocity zones of these regions is that they formed during episodes of crustal rifting believed to have occurred at some time in their geologic history. Such episodes would have brought dense mafic material into the upper crust. The Arabian Shield, by contrast, appears to have evolved by a series of island-arc collisions, a process which tends to bury the denser, higher velocity crust below a depth of 20 km.

The Colorado Plateau (Roller, 1965) shares several characteristics with the Arabian Shield. Its crustal thickness (40 km) and average upper and lower crustal velocities (6.2 and 6.8 km/s) are comparable; however, its upper crust is 5 km thicker than the Arabian Shield upper crust (average 20 km).

The average crustal velocity structure of the Arabian Shield is very near the mean of the shield and platform regions we have compared. Although the average structure is quite uniform, variations between shields, probably related to variations in age, average composition, and degree of metamorphism, are certainly apparent. The identification of these relationships will be a formidable, but fruitful, task.

SUMMARY AND CONCLUSIONS

We have interpreted a detailed seismic deep-refraction profile recorded across the major structures of the southern Arabian Precambrian Shield and well onto the Red Sea shelf and have used two-dimensional ray-tracing methods to interpret the record sections in terms of models that delineate the major first- and second-order seismic features. A comparison of these seismically defined features with surface geology and other geophysical data yields a good correlation and a consistent model of the major features of the crust.

We distinguish a complex and heterogeneous crust for the Arabian Shield, which can be divided seismically into two "layers", each approximately 20 km thick (Fig. 17). The upper crustal layer consists of material having an average velocity of 6.3 km/s, overlain by a thin lower velocity, near-surface layer. The lower crustal layer consists of an upper section 10 km thick, which has an average velocity of 6.7 km/s, and a lower section, in which the velocity increases from 6.8 to 7.3–7.8 km/s. A major lateral crustal discontinuity in both the upper and lower crust intersects the profile about 25 km northeast of shot point 2. Crustal velocities generally increase across this boundary to the northeast by about 0.2 km/s. This boundary is substantially west of the Al Amar–Idsas fault, which is generally regarded as the best candidate for a suture zone between two Precambrian blocks (Schmidt et al., 1979); we infer that the actual crustal boundary is the seismically defined one and that the Al Amar–Idsas zone may be one of a series of imbricate thrust faults that are the surface expression of the suture. The suture zone apparently extends from the Al Amar–Idsas fault almost to shot point 2. In any case, the seismic refraction data support the hypothesis that the two crustal blocks are quite different.

Another first-order lateral inhomogeneity occurs at the outcrop margin of the Precambrian Shield, where it abuts against Tertiary volcanic and volcaniclastic rocks. The thickness of the crust decreases abruptly across a zone that includes this boundary, from about 40 km beneath the Shield to about 18 km beneath the coastal plain. The crust continues to thin to a thickness of about 8 km near shot point 6. Because no major velocity discontinuity occurs across this zone, an upper crustal compositional change is not necessarily required; however, neither is it ruled out. After consideration of gravity, aeromagnetic, and surface geologic evidence, Blank et al. (in prep.) interpret the crust of the Red Sea shelf and coastal plain to be oceanic in origin.

We have identified a distinctive, high-velocity anomaly in the upper crust of the Shield, about midway between shot points 4 and 5; this anomaly correlates well with the outcrop of high-grade gneiss and amphibolite of the Khamis Mushayt gneiss (Coleman, 1973). The anomaly, which is probably the seismic expression of this extensive gneiss dome or batholithic structure, apparently penetrates the entire upper crust. A similar, although less pronounced, velocity anomaly occurs between the Al Junaynah and Nabitah fault zones; it correlates with the Al Qarah gneiss dome of Schmidt et al. (1979).

Upper crustal average velocities are higher west of the southwestern Najd fault zone; this increase probably reflects the more mafic average composition of the volcanic rocks west of the Nabitah fault zone. Two intracrustal reflectors, which have been identified at depths of about 13 km beneath the Al Junaynah and southwestern Najd fault zones, probably indicate the upper limits of extensive mafic intrusive activity within the zones.

In our interpretation velocities beneath the Mohorovičić discontinuity are about 8.0 km/s southwest of shot point 3, 8.1 km/s between shot points 3 and 2, and

about 8.2 km/s northeast of shot point 2. M-discontinuity depths decrease gradually from 43 km near shot point 1 to about 38 km between shot points 4 and 5. Finally, we distinguish two velocity discontinuities below the M-discontinuity, one at 59 km depth and another at 70 km depth.

ACKNOWLEDGMENTS

This work is the outgrowth of the efforts of a great many people who contributed to the seismic-refraction profile across the Arabian Shield. We acknowledge the assistance of over fifty people in the Saudi Arabian Mission of the U.S.G.S., Jiddah, Saudi Arabia, the Office of Earthquake Studies, U.S.G.S., Menlo Park, and the Office of International Geology, U.S.G.S., Reston, Va. It is not possible to list all of their names here; the importance of their contributions to the success of this project can only be appreciated by those who participated in the planning and execution of the experiment.

The work on which this report is based was conducted as part of a work agreement between the Saudi Arabian Directorate General of Mineral Resources and the U.S. Geological Survey.

REFERENCES

Andreasen, G.E., Petty, A.J. and Blank, H.R., 1980. Total-intensity aeromagnetic map of the Precambrian Arabian Shield, Kingdom of Saudi Arabia. Saudi Arabian Directorate General of Mineral Resources, Jiddah, scale 1 : 2,000,000.

Berry, M.J. and Fuchs, K., 1973. Crustal structure of the Superior and Grenville provinces of the northeastern Canadian Shield. Bull. Seismol. Soc. Am., 63: 1393–1432.

Blank, H.R., Healy, J.H., Roller, J., Lamson, R., Fischer, F., McClearn, R. and Allen, S., 1979. Seismic refraction profile, Kingdon of Saudi Arabia—Field operations, instrumentation, and initial results. U.S. Geol. Surv. Saudi Arabian Mission Proj. Rep. 259, 49 pp.

Blank, H.R., Mooney, W.D., Lamson, R.J., Healy, J.H. and Gettings, M.E., 1983. Crustal structure of the eastern margin of the Red Sea depression, southwest Saudi Arabia, from seismic deep-refraction observations. Unpubl. Rep. available from the U.S. Geological Survey Saudi Arabian Mission, Jiddah.

Brown, G.F., 1972. Tectonic map of the Arabian Peninsula. Saudi Arabian Dir. Gen. Miner. Resour. Arabian Peninsula Map AP-2, scale 1 : 4,000,000.

Červený, V., Molotkov, I.A. and Pšenčík, I., 1977. Ray method in seismology. The Charles University Press, Prague, 214 pp.

Coleman, R.G., 1973. Reconnaissance geology of the Khaybar quadrangle, Kingdom of Saudi Arabia. Saudi Arabian Dir. Gen. Miner. Resour., Map GM-4, 5 pp., scale 1 : 100,000.

Delfour, J., 1979. Geologic map of the Halaban quadrangle, sheet 23G, Kingdom of Saudi Arabia. Saudi Arabia, Dir. Gen. Miner. Resour., Geol. Map, GM-46A, 32 pp., scale 1 : 250,000.

Drake, C.L. and Girdler, R.W., 1964. A geophysical study of the Red Sea. Geophys. J. R. Astron. Soc., 8: 473–495.

Gettings, M.E., 1981. Status of regional gravity project, Kingdom of Saudi Arabia, as of January 1, 1979. U.S. Geol. Surv. Saudi Arabian Proj. Misc. Doc. 1 (Interagency Rep. 279), 26 pp; also, 1981, U.S. Geol. Surv., Open-File Rep., 81–165.

Gettings, M.E., 1982. Heat-flow measurements at shot points along the 1978 Saudi Arabian seismic deep-refraction line. Part 2. Discussion and interpretation. Saudi Arabian Deputy Minist. Miner. Resour., Open-File Rep., USGS-OF-02-40, 40 pp.; also, 1982, U.S. Geol. Surv. Open-File Rep., 82-794.

Gettings, M.E. and Showail, A., 1982. Heat-flow measurements at shot points along the 1978 Saudi Arabia seismic deep-refraction line. Part 1. Results of the measurements. Saudi Arabian Deputy Minist. Miner. Resour., Open-File Rep., USGS-OF-02-39, 98 pp.; also, U.S. Geol. Surv., Open-File Rep., 82-793.

Gettings, M.E., Blank, H.R., Mooney, W.D. and Healy, J.H., 1983. Crustal structure of southwestern Saudi Arabia. Saudi Arabian Deputy Minist. Miner. Resour., Open-File Rep., USGS-OF-03-59, 51 pp.; also, U.S. Geol. Surv., Open File Rep., 83-638.

Gettings, M.E., Blank, H.R., Mooney, W.D. and Healy, J.H., 1985. Crustal structure of southwestern Saudi Arabia. J. Geophys. Res., in press.

Gillmann, M., 1968. Primary results of a geological and geophysical reconnaissance of the Jizan coastal plain in Saudi Arabia. Am. Inst. Min. Metall. Eng., Soc. Pet. Geol., Saudi Arabian Sect., 2nd Reg. Symp., Dhahran, Proc., pp. 189–208.

Girdler, R.W., 1969. The Red Sea: a geophysical background. In: E.T. Degens and D.A. Ross (Editors), Hot brines and recent heavy metal deposits in the Red Sea. Springer, New York, pp. 38–58.

Greenwood, W.R., Anderson, R.E., Fleck, R.J. and Roberts, R.J., 1980. Precambrian geologic history and plate tectonic evolution of the Arabian Shield. Saudi Arabia, Dir. Gen. Miner. Resour., Bull., 24: 34 pp.

Hall, D.H. and Hajnal, Z., 1973. Deep seismic crustal studies in Manitoba. Bull. Seismol. Soc. Am., 63: 885–910.

Healy, J.H., Mooney, W.D., Blank, H.R., Gettings, M.E., Kohler, W.M., Lamson, R.J. and Leone, L.E., 1982. Saudi Arabian seismic deep-refraction profile. Final Proj. Rep., Saudi Arabian Deputy Minist. Miner. Resour., Open-File Rep., USGS-OF-02-37, 429 pp., including appendices; also, 1983, U.S. Geol. Surv., Open-File Rep., 83-390.

Hill, M.N., 1957. Recent geophysical exploration of the ocean floor. In: L.H. Ahrens, K. Rankama and S.K. Runcorn (Editors), Physics and Chemistry of the Earth, Vol. 2. Pergamon, New York, pp. 129–163.

Hill, D.P. and Pakiser, L.C., 1966. Crustal structure between the Nevada test site and Boise, Idaho, from seismic-refraction measurements. In: J.S. Steinhart and T.J. Smith (Editors), The Earth beneath the Continents. Am. Geophys. Union, Geophys. Monogr., 10: 391–419.

Hirn, A., Steinmetz, L., Kind, R. and Fuchs, K., 1973. Long range profiles in western Europe. II. Fine structure of the lower lithosphere in France (southern Bretagne). Z. Geophys., 39: 363–384.

Knopoff, L. and Fouda, A.A., 1975. Upper-mantle structure under the Arabian Peninsula. Tectonophysics, 26(1–2): 121–134.

Knott, S.T., Bunce, E.T. and Chase, R.L., 1966. Red Sea seismic reflection studies. In: T.N. Irvine (Editor), The World Rift System. Can. Geol. Surv. Pap. 66-14, pp. 33–61.

Kosminskaya, I.P., Belyaevsky, N.A. and Volvovsky, I.S., 1969. Explosion seismology in the USSR. In: P.J. Hart (Editor), The Earth's Crust and Upper Mantle. Am. Geophys. Union, Geophys. Monogr., 13: 195–208.

Kosminskaya, I.P., Puzyrev, N.N. and Alekseyev, A.S., 1972. Explosion seismology: its past, present and future. In: A.R. Ritsema (Editor), The Upper Mantle. Tectonophysics, 13: 309–323.

Le Pichon, X., Francheteau, J. and Bonnin, J., 1973. Plate Tectonics. Elsevier, Amsterdam, 302 pp.

McCamy, K. and Meyer, R.P., 1966. Crustal results of fixed multiple shots in the Mississippi embayment. In: J.S. Steinhart and T.J. Smith (Editors), The Earth beneath the Continents. Am. Geophys. Union, Geophys. Monogr., 10: 370–381.

Merghelani, H.M. and Gallanthine, S.K., 1980. Microearthquakes in the Tihamat–Asir region of Saudi Arabia. Bull. Seismol. Soc. Am., 70: 2291–2293.

Milkereit, B. and Flüh, E.R., 1985. Saudi Arabia refraction profile: Crustal structure of the Red Sea–Arabian shield transition. Tectonophysics, 111: 283–298.

Mooney, W.D., 1980. IASPEI workshop—seismic modelling of laterally varying structures (Arabian Shield to the Red Sea). EOS, Trans. Am. Geophys. Union, 61: 19.

Mooney, W.D. and Prodehl, C.A. (Editors), 1984. Proceedings of the 1980 workshop of the IASPEI on the seismic modeling of laterally varying structures: Contributions based on data from the 1978 Saudi Arabian refraction profile. U.S. Geol. Surv. Circ., 937: 158 pp.

Mooney, W.D., Andrews, M.C., Ginzburg, A., Peters, D.A. and Hamilton, R.M., 1983. Crustal structure of the northern Mississippi embayment and a comparison with other continental rift zones. Tectonophysics, 94: 327–348.

Mykkeltveit, S., 1980. A seismic profile in southern Norway. Pure Appl. Geophys., 118: 1310–1325.

Niazi, M., 1968. Crustal thickness in the Saudi Arabian Peninsula. Geophys. J. R. Astron. Soc., 15(5): 545–547.

Phillips, J.D. and Ross, D.A., 1970. Continuous seismic reflection profiles in the Red Sea. Philos. Trans. R. Soc. London, Ser. A, 267: 205–217.

Powers, R.W., Ramirez, L.F., Redmond, C.D. and Elberg, E.L., Jr., 1966. Geology of the Arabian Peninsula—Sedimentary geology of Saudi Arabia. U.S. Geol. Surv., Profess. Pap., 560-D, 147 pp.

Prodehl, C., 1985. Interpretation of a seismic-refraction survey across the Arabian Shield in western Saudi Arabia. Tectonophysics, 111: 247–282.

Raitt, R.W., 1963. The crustal rocks. In: M.N. Hill (Editor), The Sea, Vol. 3. Interscience, New York, pp. 85–102.

Roller, J.C., 1965. Crustal structure in the eastern Colorado plateau province from seismic-refraction measurement. Bull. Seismol. Soc. Am., 55: 107–119.

Schmidt, D.L., Hadley, D.G. and Stoeser, D.B., 1979. Late Proterozoic crustal history of the Arabian Shield, southern Najd province, Kingdom of Saudi Arabia. In: Evolution of Mineralization of the Arabian–Nubian Shield. King Abdulaziz Univ., Inst. Appl. Geol. Bull., 3, (2). Pergamon, Oxford–New York, pp. 41–58.

Smith, T.J., Steinhart, J.S. and Aldrich, L.T., 1966. Crustal structure under Lake Superior. In: J.S. Steinhart and T.J. Smith (Editors), The Earth beneath the Continents. Am. Geophys. Union, Geophys. Monogr., 10: 181–197.

Sollogub, V.B., 1969. Seismic crustal studies in southeastern Europe. In: P.J. Hart (Editor), The Earth's Crust and Upper Mantle. Am. Geophys. Union, Geophys. Monogr., 13: 189–195.

Steinhart, J.S. and Meyer, R.P., 1961. Explosion studies of continental structure–University of Wisconsin, 1956–1959. Carnegie Inst. Washington Publ., 622: 409 pp.

Stoeser, D.B. and Elliott, J.E., 1980. Post-orogenic peralkaline and calc-alkaline granites and associated mineralization of the Arabian Shield, Kingdom of Saudi Arabia. In: Evolution and Mineralization of the Arabian–Nubian Shield. King Abdulaziz Univ., Inst. Appl. Geol. Bull., 3(4). Pergamon, Oxford–New York, pp. 1–23.

Tramontini, C. and Davies, D., 1969. A seismic refraction survey in the Red Sea. Geophys. J.R. Astron. Soc., 17: 225–241.